VISVESVARAYA TECHNOLOGICAL UNIVERSITY

"Jnana Sangama", Belgaum-590 014

A Dissertation Project Report on

"SITE RESPONSE STUDY AND AMPLIFICATION FACTOR FOR SHALLOW BEDROCK SITES WITH SOIL-TIRE CRUMBS MIXTURE"

Submitted in partial fulfilment for the award of the degree of

BACHELOR OF ENGINEERING

IN

CIVIL ENGINEERING

BY

THEJUS L	**1CR16CV068**
A KUMARPAL	**1CR16CV001**
NAGARAJ R B	**1CR16CV036**
GOWTHAM R	**1CR16CV020**

Under the guidance of

NARESH DIXIT P S

Assistant Professor

Department of Civil Engineering

DEPARTMENT OF CIVIL ENGINEERING

CMR INSTITUTE OF TECHNOLOGY, BENGALURU – 560 037

2019-2020

CMR INSTITUTE OF TECHNOLOGY

#132, AECS Layout, ITPL Main Road, Bengaluru-560 037

DEPARTMENT OF CIVIL ENGINEERING

Certificate

Certified that the project work entitled **"*SITE RESPONSE STUDY AND AMPLIFICATION FACTOR FOR SHALLOW BEDROCK SITES WITH SOIL-TIRE CRUMBS MIXTURE*"** is a work carried out by **Mr. THEJUS L (USN 1CR16CV068), Mr. A KUMARPAL (USN 1CR16CV001), Mr. NAGARAJ R B (USN 1CR16CV036), Mr. GOWTHAM R (USN 1CR16CV020)** are bonafide students of **CMR INSTITUTE OF TECHNOLOGY** in partial fulfillment for of the requirements as a part of the curriculum, **Bachelor of Engineering in Civil Engineering,** of **Visvesvaraya Technological University, Belagavi** during the year **2019-20**. It is certified that all correction/suggestion indicated for Internal Assessment have been incorporated in the report deposited in the departmental library. The project report has been approved as it satisfies the academic requirements in respect of the project work prescribed for the Bachelor of Engineering degree

---	---
Mr. Naresh Dixit P S	**Dr. Asha M Nair**
Assist. Professor	HOD
Dept. of Civil Engineering	Dept. of Civil Engineering
CMRIT, Bengaluru	CMRIT, Bengaluru

External Viva

Name of the examiners	**Signature with date**
1.	
2.	

CMR INSTITUTE OF TECHNOLOGY

#132, AECS Layout, ITPL Main Road, Bengaluru-560 037

DEPARTMENT OF CIVIL ENGINEERING

DECLARATION

We, **Mr. Thejus L, Mr. A Kumarpal, Mr. Nagaraj R B, Mr. Gowtham R**, bonafide students of CMR Institute of Technology, Bangalore, hereby declare that dissertation entitled **"*Site Response Study and Amplification Factor for Shallow Bedrock Sites with Soil-Tire Crumbs Mixture*"** has been carried out by us under the guidance of **Mr. Naresh Dixit P S (Assistant Professor)**, Department of Civil Engineering, CMR Institute of Technology, Bangalore, in partial fulfilment of the requirement for the award of degree of Bachelor of Engineering in **Civil Engineering** of the Visvesvaraya Technological University, Belgaum during the academic year **2019-2020**. The work done in this dissertation report is original and it has not been submitted for any other degree in any university.

THEJUS L
(1CR16CV068)

A KUMARPAL
(1CR16CV001)

NAGARAJ R.B
(1CR16CV036)

GOWTHAM R
(1CR16CV020)

ABSTRACT

Unrecycled tire waste is an enormous global problem because of its non-biodegradability, flammability and chemical composition and since they are hefty and made of multiple materials, it presents distinct challenges in recycling and disposal. In 2008, around one billion tires were being produced globally each year, with an estimated further four billion already in stockpiles. The production and disposal of tires has been on the rise ever since. Due to a shortage of natural resources and increase in waste disposal cost, waste tires in the form of crumbs are widely used as a lightweight material for the backfill in embankment construction. Reduction in loss of lives due to earthquakes can be achieved by implementing safe seismic construction procedures. But the existing safe seismic methods are costly and incur an extra 15-25% of cost of the project, which is not affordable by all. Due to the damping behaviour of rubber, research has shown that waste tires in the form of crumbs can be used to reduce the vibrations and seismic isolation of buildings.

Amplification is a key parameter considered to account modification of seismic wave in the soil for earthquake resistance design of structure placed on soil. Initially, earthquake wave amplifications are related with shear wave velocity (Vs) ratio of soil and foundation layer, and then it was related to average value of Vs up to 30 m(Vs 30). Application of Vs 30 concept to represent amplification in shallow bedrock sites is questionable and has rock velocity added to soil velocity.

In this study, shallow bedrock sites in Bengaluru has been analysed. The site response calculations are done using one-dimensional non-linear approach. Intraplate recordings from around the world suitable for the study area are selected. This amplification factor represents the significant amplification of the site. Acceleration spectra show similar trends for different site classes irrespective of the fact that profiles are selected based on Vs values or SPT-N values.

Based on the results obtained it is observed that over a wide range of results indicates shear modulus as an influencing parameter. Comparison of spectral signatures for different site classes suggests that amplification reduces as the modulus of the soil column increases. Thus, it may be appropriate to classify sites based on shear modulus of soil column.

ACKNOWLEDGEMENT

The satisfaction and euphoria that accompany a successful completion of any task would be incomplete without the mention of people who made it possible, success is the epitome of hard work and perseverance, but steadfast of all is encouraging guidance.

So, with gratitude, we acknowledge all those whose guidance and encouragement served as beacon of light and crowned our effort with success.

We consider it a privilege and honour to express our sincere gratitude to our guide **Mr. Naresh Dixit P S,** Assistant Professor, Department of Civil Engineering, for his valuable guidance throughout the tenure of this final year project.

We are also thankful to **Dr. Sanjay Jain, Principal** and **Dr. Asha M. Nair, Head of Department of Civil Engineering** for their constant support and encouragement.

It's also a great pleasure to express our deepest gratitude to all faculty members of our department for their cooperation and constructive criticism offered, which helped us a lot during the project.

LIST OF FIGURES

LIST OF TABLES

CONTENTS

CHAPTER 1

1.1 Introduction

Earthquakes square measure one among the nature's most prominent perils to life and most dreaded wonder on this planet. Seismic tremors have demolished uncounted urban areas and towns on pretty much every mainland. Be that as it may, the damage caused by quakes is almost identified with artificial structures, aside from inside the instance of avalanches. Tremors cause passing by the damage they incited in structures appreciate structures, dams, extensions and elective works of man. an entire website portrayal is essential for the precarious webpage characterization. Site micro-zonation. truly, the geography way to deal with flimsy hazard has given the best need to the gauge of temperamental peril, that is,the probability that partner seismic tremor of a given greatness could happen in an exceedingly given space at interims a given measure of your opportunity. Seismic micro-zonation is subdividing a region into smaller areas having different potential for hazardous earthquake effects1. The earthquake effects depend on ground geomorphologic attributes consisting of geological, geomorphology and geotechnical information. The parameters of geology and geomorphology, soil coverage/thickness, and rock outcrop/depth are some of the important geomorphological attributes. Other attributes are the earthquake parameters, which are estimated by hazard analysis and effects of local soil for a hazard (local site response for an earthquake). The Peak Ground Acceleration (PGA) [from deterministic or probabilistic approach], amplification/ site response, predominant frequency, liquefaction and landslide due to earthquakes are some of the important seismological attributes. Weight of the attributes depends on the region and decision maker, for example flat terrain has weight of "0" value for landslide and deep soil terrain has highest weight for site response or liquefaction

An earthquake (also known as a quake**,** tremor **or** temblor) is the result of a sudden release of energy in the Earth's crust that creates seismic waves. The seismicity or seismic activity of an area refers to the frequency, type and size of earthquakes experienced over a period of time. Earthquakes are measured with a seismometer; a device which also records is known as a *seismograph.* The moment magnitude (or the related and mostly obsolete Richter magnitude) of an earthquake is conventionally reported, with magnitude 3 or lower

earthquakes being mostly imperceptible and magnitude 7 causing serious damage over large areas. Intensity of shaking is measured on the modified Mercalli scale. The depth of the earthquake also matters - shallower are the earthquakes, the more damage to structures (all else being equal.

At the Earth's surface, earthquakes manifest themselves by shaking and sometimes displacing the ground. When a large earthquake epicentre is located offshore, the seabed sometimes suffers landslides and occasionally volcanic activity. In its most sufficient displacement to cause at Tsunami. The shaking in earthquakes can also trigger generic sense, the word *earthquake* is used to describe any seismic event whether a natural phenomenon or an event caused by humans that generates seismic waves. Earthquakes are caused mostly by rupture of geological faults, but also by volcanic activity, landslides, mine blasts, and nuclear tests. An earthquake's point of initial rupture is called its focus or hypocentre. The term epicentre refers to the point at ground level directly above the hypocentre. The earthquake epicenter of Bhuj earthquake and the effect of the earthquake is shown in Fig. 1 and Fig. 2 respectively.

In its most general sense, the word earthquake is used to describe any seismic event whether natural or caused by humans that generates seismic waves. Earthquakes are caused mostly by rupture of geological faults, but also by other events such as volcanic activity, landslides, mine blasts, and nuclear tests. An earthquake's point of initial rupture is called its focus or hypocentre. The epicentre is the point at ground level directly above the hypocentre. Earthquakes are measured using measurements from seismometers

Earthquake wave may move in any direction and for design purposes, it is resolved into the vertical and horizontal directions. On an average, a value of 0.1 to 0.15g (where g = acceleration due to gravity) is generally sufficient for high dams in seismic zones. In extremely seismic regions and in conservative designs, even a value of 0.3g may sometimes by adopt.

Tectonic earthquakes occur anywhere in the earth where there is sufficient stored elastic strain energy to drive fracture propagation along a fault plane. The sides of a fault move past each other smoothly and a seismically only if there are no irregularities or asperities

along the fault surface that increase the frictional resistance. Most fault surfaces do have such asperities and this leads to a form of stick-slip behaviour. Once the fault has locked, continued relative motion between the plates leads to increasing stress and therefore, stored strain energy in the volume around the fault surface. This continues until the stress has risen sufficiently to break through the asperity, suddenly allowing sliding over the locked portion of the fault, releasing the energy. This energy is released as a combination of radiated elastic strain seismic, frictional heating of the fault surface, and cracking of the rock, thus causing an earthquake. This process of gradual build-up of strain and stress punctuated by occasional sudden earthquake failure is referred to as the elastic-rebound theory. It is estimated that only 10 percent or less of an earthquake's total energy is radiated as seismic energy. Most of the earthquake's energy is used to power the earthquake fracture growth or is converted into heat generated by friction. Therefore, earthquakes lower the Earth's available elastic potential energy and raise its temperature, though these changes are negligible compared to the conductive and convective flow of heat out from the Earth's deep interior.

There are three main types of fault, all of which may cause an inter plate earthquake: normal, reverse (thrust) and strike-slip. Normal and reverse faulting are examples of dip-slip, where the displacement along the fault is in the direction of dip and movement on them involves a vertical component. Normal faults occur mainly in areas where the crust is being extended such as a divergent boundary. Reverse faults occur in areas where the crust is being shortened such as at a convergent boundary. Strike-slip faults are steep structures where the two sides of the fault slip horizontally past each other; transform boundaries are a particular type of strike-slip fault. Many earthquakes are caused by movement on faults that have components of both dip-slip and strike-slip; this is known as oblique slip.

The most important parameter controlling the maximum earthquake magnitude on a fault is however not the maximum available length, but the available width because the latter varies by a factor of 20. Along converging plate margins, the dip angle of the rupture plane is very shallow, typically about 10 degrees. Thus, the width of the plane within the top

brittle crust of the Earth can become 50 to 100 km making the most powerful earthquakes possible.

Fig. 1 Earthquake epi-centre of Bhuj Earthquake

Fig. 2 Effect of Bhuj earthquake on building

Strike-slip faults tend to be oriented near vertically, resulting in an approximate width of 10 km within the brittle crust, thus earthquakes with magnitudes much larger than 8 are not possible. Maximum magnitudes along many normal faults are even more limited because many of them are located along spreading centres, as in Iceland, where the thickness of the brittle layer is only about 6 km.

In addition, there exists a hierarchy of stress level in the three fault types. Thrust faults are generated by the highest, strike slip by intermediate and normal faults by the lowest stress levels. This can easily be understood by considering the direction of the greatest principal stress, the direction of the force that 'pushes' the rock mass during the faulting. In the case of normal faults, the rock mass is pushed down in a vertical direction, thus the pushing force (greatest principal stress) equals the weight of the rock mass itself. In the case of thrusting, the rock mass 'escapes' in the direction of the least principal stress, namely upward, lifting the rock mass up, thus the overburden equals the least principal stress. Strike-slip faulting is intermediate between the other two types described above. This difference in stress regime in the three faulting environments can contribute to differences in stress drop during faulting, which contributes to differences in the radiated energy, regardless of fault dimensions.

1.2 Earthquake zones in India

The latest version of seismic zoning map of India given in the earthquake resistant design code of India [IS 1893 (Part 1) 2002] assigns four levels of seismicity for India in terms of zone factors. In other words, the earthquake zoning map of India divides India into 4 seismic zones (Zone 2, 3, 4 and 5) unlike its previous version, which consisted of five or six zones for the country. This is shown in Fig. 3 . According to the present zoning map, Zone 5 expects the highest level of seismicity whereas Zone 2 is associated with the lowest level of seismicity.

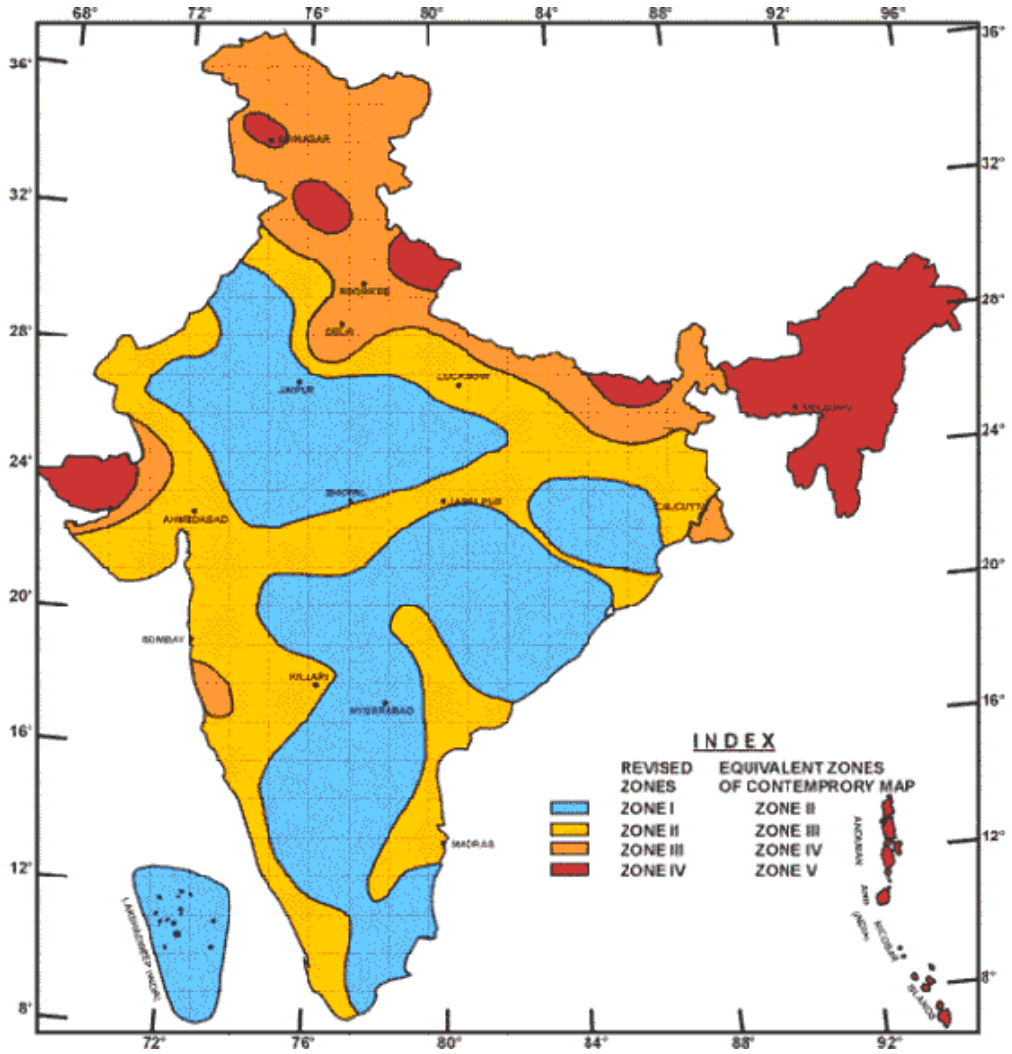

Fig. 3: Earthquake hazard zoning map of India

Zone 5

Zone 5 covers the areas with the highest risks zone that suffers earthquakes of intensity MSK IX or greater. The IS code assigns zone factor of 0.36 for Zone 5. Structural designers use this factor for earthquake resistant design of structures in Zone 5. The zone factor of 0.36 is indicative of effective (zero periods) level earthquake in this zone. It is referred to as the Very High Damage Risk Zone. The region of Kashmir, the western and central Himalayas, North and Middle Bihar, the North-East Indian region and the Rann of Kutch fall in this zone. Generally, the areas having trap rock or basaltic rock are prone to earthquakes.

Zone 4

This zone is called the High Damage Risk Zone and covers areas liable to MSK VIII. The IS code assigns zone factor of 0.24 for Zone 4. The Indo-Gangetic basin and the capital of the country (Delhi), Jammu and Kashmir fall in Zone 4. In Maharashtra, the Patna area (Koyana nager) is also in zone no-4. In Bihar the northern part of the state like- Raksaul, near the border of India and Nepal, is also in zone no-4.

Zone 3

The Andaman and Nicobar Islands, parts of Kashmir, Western Himalayas fall under this zone. This zone is classified as Moderate Damage Risk Zone which is liable to MSK VII and also 7.8 The IS code assigns zone factor of 0.16 for Zone 3.

Zone 2

This region is liable to MSK VI or less and is classified as the Low Damage Risk Zone. The IS code assigns zone factor of 0.10 (maximum horizontal acceleration that can be experienced by a structure in this zone is 10% of gravitational acceleration) for Zone 2.

1.3 Seismic micro-zonation:

It is defined as the process of subdividing a potential seismic or earthquake prone area into zones with respect to some geological and geophysical characteristics of the sites such as ground shaking, liquefaction susceptibility, landslide and rock fall hazard, earthquake-related flooding, so that seismic hazards at different locations within the area can correctly be identified. Micro-zonation provides the basis for site-specific risk analysis, which can assist in the mitigation of earthquake damage. In most general terms, seismic micro-zonation is the process of estimating the response of soil layers under earthquake excitations and thus the variation of earthquake characteristics on the ground surface.

Regional geology can have a large effect on the characteristics of ground motion. The site response of the ground motion may vary in different locations of the city according to the local geology. A seismic zonation map for a whole country may, therefore, be inadequate for detailed seismic hazard assessment of the cities. This necessitates the development of micro-zonation maps for big cities for detailed seismic hazard analysis. Micro-zonation

maps can serve as a basis for evaluating site-specific risk analysis, which is essential for critical structures like nuclear power plants, subways, bridges, elevated highways, sky trains and dam sites. Seismic micro-zonation can be considered as the preliminary phase of earthquake risk mitigation studies. It requires multi-disciplinary contributions as well as comprehensive understanding of the effects of earthquake generated ground motions on manmade structures. Many large cities around the world have put effort into developing micro-zonation maps for the better understanding of earthquake hazard within the cities.

1.4 Earthquake Ground Response Analysis

The local soil conditions have a profound influence on ground response during earthquakes. The recent destructive earthquakes have demonstrated that the topography, nature of the bedrock and nature and geometry of the depositional soils are the primary factors that influence local modifications to the underlying motion. For example, earthquakes in Mexico (1985) and Loma Prieta (1989) have demonstrated the significant effect of local soil conditions on the ground motion parameters. In Mexico earthquake, ground motion in the lakebed zone was amplified 8 to 50 times with respect to rock zone (Gaull et al., 1995). In stable soils, the seismic waves can propagate through the soil without appreciable loss of shear strength. But the ground motion parameters will be modified depending up on local soil conditions. However, in unstable soils significant loss of shear strength occurs and produces failure such as in the case of liquefaction, large settlement and landslide (Mohamedzein et al, 2006).

1.4.1 Site Specific Ground Response Analysis

The very basic problem to be solved by geotechnical engineers in regions where earthquake hazards exist is to estimate the site-specific dynamic response of a layered soil deposit. The problem is commonly referred to as a site-specific response analysis or soil amplification study (although ground motions may be de-amplified). This is generally the beginning point for most seismic studies and a solution to this problem allows the geotechnical engineer to:

- Calculate site natural periods.

- Assess ground motion amplification.
- Provide structural engineers with various parameters, primarily response spectra, for design and safety evaluation of structures.
- Evaluate the potential for liquefaction.
- Conduct first analytical phase of seismic stability evaluations for slopes and embankments.

Soil conditions and local geological features affecting the ground response are numerous. Some of the more important features are horizontal extent and depth of the soil deposits overlying bedrock, slopes of the bedding planes of the soils overlying bedrock, changes of soil types horizontally, topography of both bedrock and deposited soils and faults crossing the soil deposits.

1.4.2 Complete ground response analysis

Ideally, a complete ground response analysis should take into account the following factors:

- Rupture mechanism at source of an earthquake (source).
- Propagation of stress waves through the crust to the top of bedrock beneath thesite of interest (path).
- How ground surface motion is influenced by the soils that lie above the bedrock (site amplification). In reality, several difficulties arise and uncertainties exist in taking in to account the above listed factors:
- Mechanism of fault rupture is very complicated and difficult to predict in advance.
- Crustal velocity and damping characteristics are generally poorly known.
- Nature of energy transmission between the source and site is uncertain. In professional practice, the following procedures are usually adopted to make the process tractable and overcome the above difficulties:

- Seismic hazard analyses (probabilistic or deterministic) are used to predict bedrock motions at the location of the site.
- Seismic hazard analyses rely on empirical attenuation relationships to predict bedrock motion parameters.

Ground response problem becomes one of determining responses of soil deposit to the motion of the underlying bedrock.

1.4.3 Selection of Rock Motions

Appropriate rock motions (either natural or synthetic acceleration time histories) are selected to represent the design rock motion for the site. The rock motion should be associated with the specific seism tectonic structures, source areas or provinces that would cause most severe vibratory ground motion or foundation dislocation capable of being produced at the site under currently known tectonic framework. Here an interaction with a seismologist is required. If natural time histories are used, it is preferable to use asset of natural time histories that have ground motion characteristics similar to those estimated for the design rock motions.

This means that the selected histories should have:

- Peak ground motion parameters
- Response spectral content and
- Duration of strong shaking

In the absence of natural motions, artificial motions can be generated using the concept of spectrum compatible time histories. For this problem several procedures are available such as time domain, frequency domain generation, empirical Green's function technique, ARMA modelling, etc.

1.4.4 Ground Response Analysis and Design Spectra

Ground response analysis, usually in the form of one-dimensional analysis (linear, equivalent linear or nonlinear) are performed for the site-specific profiles using the

rock motions as input motion, to compute the time histories at the ground surface. Response spectra of calculated ground surface motions are statically analyzed or interpreted in some manner to develop design spectrum for the site. The time histories from the ground response analysis can be used directly to represent the ground surface motions or artificial time histories can be developed to match the design spectrum.

1.4.5 Wave Propagation Analysis / Site Amplification

During earthquakes, the ground motion parameters such as amplitude of motion, frequency content and duration of the ground motion change as the seismic waves propagate through overlying soil and reach the ground surface. The phenomenon, wherein the local soils act as a filter and modify the ground motion characteristics, is known as "soil amplification problem". Physically, the problem is to predict the characteristics of the seismic motions that can be expected at the surface (or at any depth) of a soil stratum. Mathematically, the problem is one of the wave propagations in continuous medium. Excitation of a compliant medium (for example, a soil deposit or an earth dam) is not instantly felt at other points within the medium. It takes time for the effects of the excitation to be felt at distant/different points. The effects are felt in the form of waves that travel through the medium. The way these waves travel is a function of the stiffness and attenuation characteristics of the medium and will control the effects they produce. Usually, the geological materials are treated as continua and the dynamic response of these materials to dynamic/transient loading such as earthquakes, blasts, traffic-induced vibrations, etc. are evaluated in the context of one or two or three-dimensional wave propagations depending on the geometry and loading conditions.

1.4.6 One-Dimensional Wave Propagation Analysis

These are widely used for ground response analysis or soil amplification studies as:

- They are believed to provide conservative results.
- Many commercial programs with different soil models are available for use on personal computers.

- They are time tested, i.e. most design projects in the past designed using this methodology survived the earthquakes.

1.4.7 Assumptions in One-Dimensional Ground Response Analysis and Justification for Its Use

The main assumptions include

- The soil layers are horizontal and extend to infinity.
- The ground surface is level. The incident earthquakes motions are spatially uniform, horizontally polarized shear waves, and propagate vertically. In the areas of strong earthquake motion, the stress waves, from the earthquake focus are propagating nearly vertically when they arrive at the earth's surface. Wave velocity generally decreases from the earth's interior towards the surface, and hence stress waves from the focus are bent by successive refractions into a nearly vertical path.
- Even if the waves within the firm ground are propagating in a shallow inclined direction, the waves set up within the soil by refraction at the interface between the firm ground and soil will propagate nearly vertically (by Snell's law of refraction).
- Vertical ground motions are generally not as important from the standpoint of structural design as horizontal ground motions.
- Soil properties generally vary more rapidly in the vertical direction than in the horizontal direction.

A complete ground response analysis must consider the various factors mentioned before including the additional factors such as rupture mechanism at the origin of earthquake, propagation of seismic waves through the crust to the top of bedrock. These factors are difficult to quantify and hence a complete ground response analysis becomes highly complicated. Therefore, one-dimensional ground response analyses are used extensively due to their simplicity.

1.4.8 Methods of Ground Response Analysis

A number of techniques are available for „ground response analyses. The methods differing the simplifying assumptions that are made, in the representation of stress–strain relations of soil and in the methods used to integrate the equation of motion. The development of existing methods of dynamic response analysis has been a gradual evolutionary process stimulated by changing needs of practice and the increasing knowledge about the fundamental behavior of soils under cyclic loading derived from field observations and laboratory testing. The method can be broadly grouped into the following three categories:

(a) Linear analysis.

(b) Equivalent linear analysis.

(c) Nonlinear analysis

(a) Linear analysis: Linear analysis, because of its simplicity, has been extensively used study analytically the dynamic response of soil deposits. Closed form analytical solutions have been derived for idealized geometries and soil properties e.g. by assuming that the deposit consists of one uniform layer with soil stiffness either constant or varying with depth in a way which can be expressed by simple mathematical functions. In general, however, soil does not behave elastically, and its material properties can change in space. In such situations, no analytical solutions are possible and numerical techniques such as finite element or finite difference method are used.

(b) Equivalent linear analysis: Schnabel et al. addressed nonlinear hysteretic stress–strain properties of sand by using an equivalent linear method of analysis. The method was originally based on the lumped mass model of sand deposits resting on rigid base to which the seismic motions were applied. Later, this method was generalized to wave propagation model with an energy-transmitting boundary. The seismic excitation could be applied at any level in the new model.

(c) Nonlinear analysis. A nonlinear analysis is usually performed by using a discrete model such as finite element and lumped mass models and performing time domain step by-step integration of equations of motion. For nonlinear analysis to give meaningful results, the stress– strain characteristics of the particular soil must be realistically modelled. In the present study the parameters of interest in the seismic response analysis involves the fundamental frequency of the soil layers, time history of ground motion parameters at the ground surface and response spectra. These parameters are evaluated using the computer programme DEEPSOIL V6.1 based on equivalent linear approach. The input parameter for the model such as shear wave velocity of each soil layer has been obtained from the empirical relation proposed by Japanese Road Association as proposed by **Lee, (1992)** as below.

Vs = 80 N1/3 m/s for sands

Vs = 100 N1/3 m/s for **clays**

Where **N** = **SPT 'N'** Value, **Vs** = Shear velocity

To account for soil behavior under irregular cyclic loading, the dynamic properties of soils such as modulus reduction and damping versus shear strain curves proposed by **Vucetic** and **Dobry (1991)** were used based on plasticity characteristics of respective soil layers in various soil profiles.

1.4.9 Selection of Peak Ground Acceleration and Input Earthquake Motion

Appropriate rock motions (either natural or synthetic acceleration time histories) are selected to represent the design rock motion for the site. The rock motion should be associated with the specific seism tectonic structures, source areas or provinces that would cause most severe ground motion at the site under currently known tectonic framework. In seismically active regions it may be possible to reduce earthquake damage by conducting detailed specific prediction of seismic ground motion. With the knowledge of earthquake source mechanisms and path effects, detailed ground motion at any specific site of interest may be determined without waiting for the earthquakes to occur. This approach is of great importance, especially in the regions

where ground motion records of engineering interest are totally absent. In the absence of recorded motions, artificial motions can be generated.

1.4.9.1 Peak Ground Acceleration

According to seismic hazard map of India, Bureau of Indian Standards (IS 1893: 2002), Bangalore is located in Zone II with zone factor 0.07. In this area, no seismic recording stations were established and consequently no records of strong ground motion are available. Therefore, the design ground motion parameter for the study area has been obtained from Global Seismic Hazard Assessment Programme (GSHAP) map which is based on 10% probability of exceedance in 50 years and by Attenuation relation from Iyengar and Raghukanth (2004) In this, we can calculate horizontal peak ground acceleration at a site in Peninsular India using attenuation relationships for Hypo central Depth taken as 10.0 Km and the relation is valid over the range of 10 to 300 km for rock sites only. Hence the corresponding maximum peak ground acceleration (PGA) of 0.1g has been selected for Bangalore region.

1.4.9.2 Generation of Artificial or Synthetic Earthquake Motions at the Bed Rock

For a deep profile overlaying the bedrock, the profile is divided into rock layers and soil layers. Given a moment magnitude and an epicentre distance, using various computer models one can generate an acceleration time history at the outcrop of a rock site. Then performing a site response analysis one can generate an acceleration time history at the ground surface.

1.4.10 Strong Motion Characteristics

1.4.10.1 Peak Ground Acceleration

The earthquake time history contains several engineering characteristics of ground motion and maximum amplitude of motion is one of the important parameters among them. The PGA is a measure of maximum amplitude of motion and is defined as the largest absolute value of acceleration time history. The response of very stiff structures (i.e., with high frequency) is related to PGA. Though PGA is not a very good measure of damage potential of ground motion; due to its close relation with response spectrum

and usability in scaling of response spectrum, PGA is extensively used in engineering applications. Generally, at distances several source dimensions away, vertical PGAs are found to be less than horizontal PGA though at near source distances it could be equal to higher than the corresponding horizontal PGA. For engineering purposes, vertical PGA is assumed to be two thirds of the horizontal PGA.

1.4.10.2 Peak Velocity

Peak velocity is the largest absolute value of velocity time history. It is more sensitive to the intermediate frequency components of motion and characterizes the response to structures that are sensitive to intermediate range of ground motions, e.g. tall buildings, bridges, etc.

1.4.10.3 Peak Displacement

Peak displacements reflect the amplitude of lower frequency components in ground motion. Accurate estimation of these parameters is difficult as the errors in signal processing and numerical integration greatly affect the estimation of amplitude of displacement time history.

1.4.11 CHA

Illustration of generation of synthetic ground motion is shown in Fig. 4. The most commonly used methods for generation of artificial ground motions fall into four main categories:

(a) Modification of actual ground motion records

(b) Generation of artificial motions in the time domain

(c) Generation of artificial motions in the frequency domain

(d) Generations of artificial motions using Green's functions techniques.

(a) Modification of actual ground motion records

Perhaps the simplest approach to the generation of artificial ground motions is the modification of actual recorded ground motions. Maximum motion levels, such as

peak acceleration and peak velocity, have been used to rescale actual strong motion

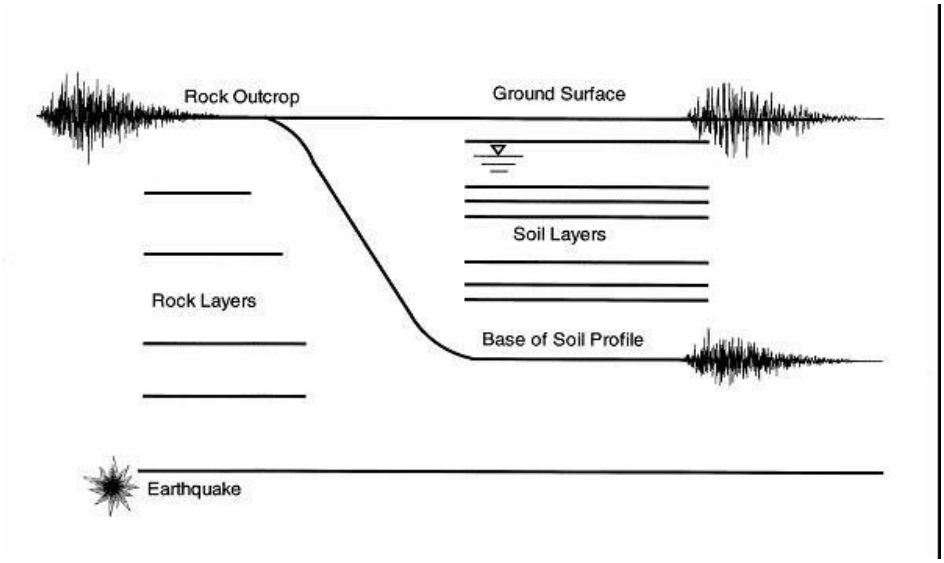

Fig. 4 Illustration of Generating Synthetic Ground Motions

records to higher or lower levels of shaking (Figure 4). Krinitszky and Chang recommended that the scaling factor (the ratio of the target amplitude to the amplitude of the record being scaled) should be kept as close to 1 as possible, and always between **0.25** and **4.0**, and that analyses be conducted with several scaled records.

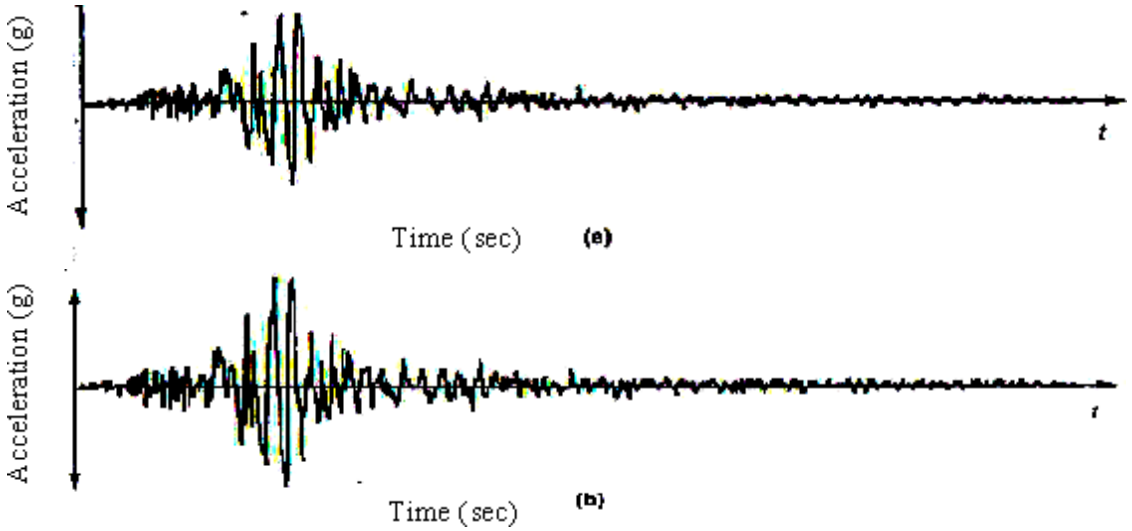

Fig. 5 Example of time –domain generation of synthetic time history **(a)** time history of white noise is filtered in the time domain to produce **(b)**

Vanmarcke noting that simple amplitude scaling fails to account for differences in important characteristics such as frequency content and duration, suggested that limits on the scaling factor should be related to the type of problem to which the resulting motion is to be applied. For analysis of linear elastic structures, the limits of **Krinitszky** and **Chang** were considered suitable, but for liquefaction a scaling factor range of 0.5 to 2.0 was recommended.

Frequency domain generation

Ground motions can be generated quite conveniently in the frequency domain by combining a Fourier amplitude spectrum with a Fourier phase spectrum. The amplitude spectrum may be computed from an actual ground motion spectrum or may be represented by some theoretical means, such as a Brune spectrum or a power spectral density function .The phase spectrum may be obtained from an actual ground motion or may be computed from a time history given by the product of white noise and an envelope function. Frequency – domain methods are particularly useful for

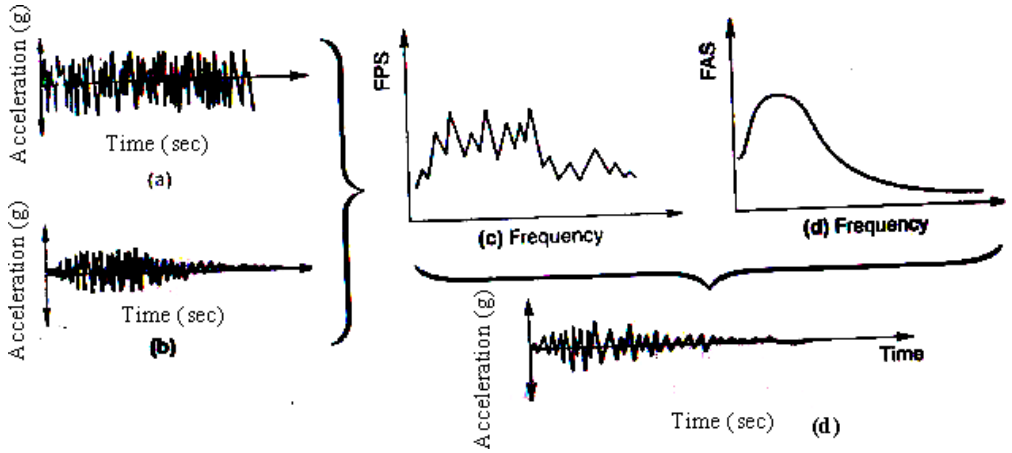

Fig. 6 Example of frequency-domain generation of synthetic time history: **(a)** time history of white noise is shaped by envelope function to produce **(b)** time history of enveloped white noise. Fourier transform of enveloped white noise is performed to obtain **(c)** Phase spectrum is combined with **(d)** amplitude spectrum to produce **(e)** synthetic time history.

generation motions that are consistent with target response spectra. Computer programs such as EQGEN and PASCAL assume initial Fourier amplitude and phase spectra, and then iteratively adjust the ordinates of the Fourier amplitude spectrum

until a motion consistent with the target response spectrum is produced. The origin of the target response spectrum must be kept in mind when generating spectrum compatible motions. An example of frequency domain generation of synthetic time history is shown in Fig. 6.

Green's function technique

The Green's function approach to ground motion modeling is based on the idea that the total motion at a particular site is equal to the sum of the motions produced by a series of individual ruptures of many small patches on the causative fault. Obtaining the site motion requires defining the geometry of the earthquake sources, dividing the source into a finite number of patches, defining the sequence in which the patches rupture, defining the slip functions(functions describing the variation of slip displacement with time for each patch) across the source , and defining Green's functions (functions that describe the motion at the site due to an instantaneous unit slip at the source see Figure 6 across the source .Combining the Green's function with the slip function gives the motion at the site due to slip of each individual patch. Summing the effects of the slips of each patch while accounting for the order in which they rupture produces the overall ground motion at the site. Obviously, the summation procedure assumes that all materials remain linear. The schematic of generation of motion using Green's function technique is shown in Fig. 7.

Calculation of Green's functions requires knowledge of the velocity structure of the crustal materials between the source and site. Considerable computational effort is also required to calculate Green's function; finite-element, finite difference, and ray theory techniques are usually used for this purpose. Hartzell (1978) bypassed these computations by using the weak motions of small earthquakes as empirical Green's functions to simulate the strong motion of large earthquakes. Empirical Green's functions have the benefit of automatically retaining the effects of the crustal velocity structure. The Green's function approach is particularly useful for generating near-field motions, that is, motions at sites close enough to the fault that the fault dimensions become significant (for far-field sites, the field can be treated as a point source without undue loss of accuracy).

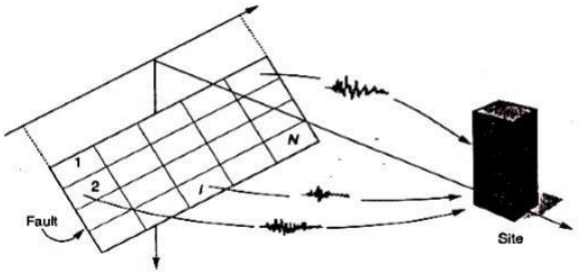

Fig. 7 Schematic of Green's functions for a fault divided into N patches. Differences in the Green's functions for the different patches are due to differences in focal length, epicentral distance, and geologic structure along the source –site path. Once Green's functions determined, site motions can easily be simulated for a variety of fault rupture patterns and slip functions.

CHAPTER 2

2.1 LITERATURE REVIEW

1. **P. Anbazhagan, D.R. Manohar (January 2015) – 'Energy Absorption Capacity and Shear Strength Characteristics of Waste Tire Crumbs and Sand Mixtures'**

   The primary objective of the study was to estimate the energy absorption (EA) capacity, brittleness index (ductility) and stiffness characteristics of Sand-Tire Crumb Mixtures (STCM) using direct shear test and Unconsolidated Undrained (UU) triaxial test for the effective reuse of waste tire crumbs as isolation materials. Direct shear test as per ASTM-D5321 (2008) and static triaxial test as per ASTM-D2850 (2007). It was found that the shear strength enhancement by adding rubber crumbs increases with the percentage of rubber and starts decreasing after 25% rubber by volume. The strength characteristics of sand were increased by the inclusion of rubber, which in turn increase the energy absorption capacity and ductility.

   It was concluded from this study that the addition of waste tire crumbs to sand increases the energy absorption capacity and ductility by about 40 to 70%.

2. **Anbazhagan Panjamani, Tsang Hing Ho, Manohar D. R. (June 2015) – 'Shear strength characteristics and static response of sand-tire crumb mixtures for seismic isolation'**

   The objective of this study was to investigate the shear strength characteristics, energy absorption capacity and brittleness index of sand-tire crumb mixtures using simple direct shear test and Unconsolidated Undrained (UU) triaxial test for the effective use of waste tire crumbs for seismic isolation of building. Direct shear test was as per ASTM-D5321 (2008) and static triaxial test was as per ASTM-D2850(2007).

   The optimal size of rubber selected for this study was 5.6 mm, with 25% tire crumbs by volume. The addition of tire crumbs to sand significantly increased peak shear strength, improved friction angle from 32^{o} to 46^{o}, reduced brittleness index and increased energy absorption capacity by about 50% compared to that of sand for all

confining pressures. It was concluded that the shear strength and initial friction angle were significant for mixtures with 25% rubber of any size.

3. **M. Neaz Sheikh (et.al) (October 2013) – 'Shear and Compressibility Behaviour of Sand–Tire Crumb Mixtures'**

   This paper investigated the shear and compressibility behaviour of sand–tire crumb (S-TC) mixtures for their application in civil engineering projects. Triaxial and compression tests were conducted on Sand-tire crumb mixtures, where content of tire crumbs varied from 0-40% by volume. It was found that the peak shear strength and the corresponding axial strain of the mixture increased with the increase in the confining pressure. All mixtures with a percentage of tire crumbs equal to or greater than 10% showed a Brittleness Index (BI) of at least one third of the value of pure sand, indicating a ductile material. The compressibility tests showed that the high compressibility of rubber is inherited in S-TC mixtures, resulting in higher settlements.

4. **Mahmoud Ghazavi (June 2003) – 'Shear strength characteristics of sand mixed with granular rubber'**

   The main aim of the tests was to investigate the influence of the particles on shear strength parameters of rubber grain-sand mixtures. Grain size distribution, Specific gravity and Direct shear test on samples were done based on ASTM provisions. It was found that an apparent cohesion was obtained in samples containing rubber grains. It was shown that an addition of 10–20% rubber to the sand is optimal to obtain the greatest friction angle. The shear strength did not change significantly. Dilation characteristics were observed in sand-rubber mixtures, especially in samples having greater rubber content and more compaction.

5. **J. H. Lee, R. Salgado, A. Bernal and C. W. Lovell – 'Shredded tires and rubber-sand as lightweight backfill'**

   In the present paper, a laboratory study is used for a preliminary assessment of the mechanical properties of tire chips and rubber-sand (a mixture of sand and tire chips or shreds). The results are compared with previous work on similar materials. The properties are then used in the numerical modelling of a full-scale test wall with a tire-shred backfill. Experimental and numerical results are compared. Rubber-sand

samples in this study have 40% tire chips by weight. The laboratory test results were used to establish the parameters required for the hyperbolic modelling of these materials. A finite-element analysis was conducted to model the performance of tire-shred and rubber-sand backfills, and geotextile reinforced backfills under at-rest and active conditions. The results were compared with field tests performed by Tweedieet al. (1998) at the University of Maine. The finite-element analyses produced reasonably good estimates of deformations and stresses for a tire-shred backfill under at-rest condition, while showing overestimation for the active condition. In addition, the analyses indicated that the performance of rubber-sand, being both lightweight and reasonably strong, compared well with that of a sandy gravel, as a backfill material.

6. **Anbazhagan, P, Anjali Uday , Sayed S.R. Moustafa and Nassir S.N. Al-Arifi – 'Soil Void Ratio Correlation with Shear Wave Velocities and SPT N Values for Indo-Gangetic Basin'**

   In this study attempt has been made to understand in-situ void ratio in Indo-Gangetic basin (IGB) and to form empirical relations between void ratio and shear wave velocity (Vs) , N values considering subsoil investigation data. Multichannel analysis of surface wave (MASW) test and standard penetration test was carried out along with soil property measured at 25 locations. The general soil profile varied from silty sand to clay of low compressibility, ground water level fluctuated between 1-27 m, depth of borehole varied from 20-40 m. Regression analysis was conducted on 202 data sets of void ratio and shear wave velocity, 293 data sets of void ratio and SPT- N value, which resulted in inverse correlations between void ratio and Vs , SPT N value. The datas were segregated into fine, coarse grained data based on engineering classification and relations were developed separately. Until now, no studies have related in-situ void ratio to Vs and SPT N. These correlations will be useful to predict void ratio for sites having measured values of Vs and N value.

   SPT based empirical correlations are being developed worldwide due to longtime and comprehensive data accumulations. rrThis correlation are well related with index properties such as SPT N versus relative density and SPT N versus difference in the void ratio (emax – emin).

In this study, the borehole data were further used to develop relationships between void ratios and SPT N values. About 293 data points of void ratio and SPT N values were arrived from 84 borehole data.

7. **Anbazhagan Pajamani, Manohar Devarahalli Ramegowda and Divyesh Rohit – 'Low cost damping scheme for low to medium rise buildings using rubber soil mixtures'**

   This study presents the detailed results of experimental investigation to select the optimum size of tyre crumb from seven crumb sizes. Crumb size F is considered as optimum size based on shear strength, energy absorption capacity and stiffness compared to other crumb sizes. For the selected crumb size with higher rubber content numerical studies were carried out. Through numerical studies, it was noticed that percentage of rubber in RSM, thickness and width of RSM around the footing and frequency variation of the input motion are the main factors which controls the damping characteristics of earthquake motion.

8. **Mahmoud Ghazavi and Masoud Amel Sakhi – 'Influence of Optimized Tire Shreds on Shear Strength Parameters of Sand'**

   The influence of dimensions of rectangular shreds prepared from waste tires onthe shear resistance of sand shred mixtures has been investigated by performing large direct shear tests. Sand 2, 3, & 4cm width and various aspect ratios were tested at two different compaction levels. It has been found that shred contents, shred width, shred aspect ratio for given width, compaction and normal stress are influencing factors on shear strength of the mixtures. Dilation characteristics were observed in sand shred mixtures, especially in samples having greater shred content and more compaction. In almost all envelopes Mohr circle is non-linear. The friction angle of mixtures increases by using optimum shred aspect ratio and by increasing shred contents and mixture compaction. The tire shreds caused pi to be increased by about 10-94%, depending upon shred width and aspect ratio, shred content and mixture compaction.

9. **F. Farrokhzad & A. J. Choobbasti – 'Empirical correlations of shear wave velocity (Vs) and standard penetration resistance based on soil type in Babol city'**

The aim of this paper is to generate new correlations between shear wave velocity and SPT-N60 values by combining the new data obtained by authors and old available data of Babol city. A detailed site characterization of Babol city is carried out by conducting several SPT and downhole tests in an area of 35 km2. Shear wave velocities in 35 boreholes were measured to provide data for evaluation of local site effects and assessment of liquefaction potential as a part of microzonation study.

Seismic measurements of compressional and shear wave velocities are of particular importance in assessment of the engineering properties of the ground, as they can be used to determine geotechnical properties of soil, evaluation of liquefaction and analysis of local site effects during an earthquake. Good planning for a geotechnical and geophysical site investigation is the key to obtaining sufficient data with acceptable accuracy for seismic microzonation in a timely manner and with minimum cost. Most of the correlations between shear wave velocity and SPT-N values are results of case studies based on the field tests in a specific area; so, the direct application of the derived correlations for another region may require some changes in original equation.

Table 1 Literature Review

Author(s)	Journal name	About the Journal
P. Anbazhagan, D. R. Manohar	Energy Absorption Capacity and Shear Strength Characteristics of Waste Tire Crumbs and Sand Mixtures	The primary objective of the study is to estimate the energy absorption (EA) capacity, brittleness index (ductility) and stiffness characteristics of Sand-Tire Crumb Mixtures (STCM) using direct shear test and Unconsolidated Undrained (UU) triaxial test for the effective reuse of waste tire crumbs as isolation material. Direct shear test apparatus with rectangular mould having a size of 60 mm x 60 mm and thickness of 30 mm; Tests have been carried out as per ASTM-D5321 (2008) for three normal stresses of 50, 100 and 150 kPa at a constant strain rate of 0.25 mm/min. The static triaxial test was carried out as per ASTM-D2850 (2007) with a sample size of 38 mm in diameter and 76 mm in height for effective confining pressures of 20, 60 and 100 kPa at constant strain rate of 1.25 mm/min. The shear enhancement by adding rubber crumbs increases with the percentage of rubber and starts decreasing after 25% rubber by volume. The strength characteristics of sand were increased by the inclusion of rubber, which in turn increase the energy absorption capacity and ductility. It can be concluded from this study that the addition of waste tire crumbs to sand increases the energy absorption capacity and ductility by about 40 to 70%.

Anbazhagan Panjamani, Tsang Hing.Ho.	Shear strength characteristics and static response of sand-tire crumb mixtures for seismic isolation	The objective of this study is to investigate the shear strength characteristics, energy absorption capacity and brittleness index of sand-tire crumb mixtures using simple direct shear test and Unconsolidated Undrained (UU) triaxial test for the effective use of waste tire crumbs for seismic isolation of building. Direct shear test apparatus with rectangular mould having a size of 60 mm x 60 mm and thickness of 30 mm; Tests have been carried out as per ASTM-D5321 (2008) for three normal stresses of 50, 100 and 150 kPa at a constant strain rate of 0.25 mm/min. The static triaxial test was carried out as per ASTM-D2850 (2007) with a sample size of 38 mm in diameter and 76 mm in height for effective confining pressures of 20, 60 and 100 kPa at constant strain rate of 1.25 mm/min. The prepared STCM samples were poured into vacuum split mould in 4 to 5 layers to achieve uniform mixing, and were slightly compacted for higher percentage of rubber. In present study, the optimal size of rubber is 5.6 mm, with 25% by volume. The addition of tire crumbs to sand significantly increased peak shear strength. Addition of tire crumbs consistently improved friction angle from 32o to 46o. For 25% rubber content with rubber size of 5.60 mm, it is observed that a reduction of brittleness index and an increase in energy absorption capacity by about 50% compared to that of sand for all confining pressures. Maximum efficiency of STCM for different sizes of rubber is observed for crumb size of 5.60 mm, followed by 1.00 mm, 4.75 mm, and 2.00 mm. Maximum friction was obtained for 5.60 mm and 1.00 mm. It can be concluded that the shear strength and initial friction angle are significant for mixtures with 25% rubber of any size.
Horace Moo-Young; Kassahun Sellasie; Daniel Zeroka; and Gajanan Sabnis	Physical and Chemical Properties of Recycled Tire Shreds for Use in Construction	The purpose of this study was to determine the physical and chemical properties of tire shreds for use in engineering construction as a replacement for aggregates in embankments or as backfill. Testing of the physical properties of tire shreds followed the following American Society of Testing and Materials (ASTM) procedures: Absorption-ASTM C 128; Specific gravity-ASTM C 128;Permeability-ASTM D 2434; Gradation-ASTM D 422; Exposed wires-ASTM D 6270; Compaction-ASTM D 698 ~60% of Standard Test Method! and D 1557 ~Modified!; Compression- ASTM D 2166; and Shear strength-ASTM D 3080. Testing for chemical properties such as pH, turbidity, total organic carbon (TOC), and iron of tire shreds followed procedures outlined in the Standard Methods for the Examination of Water and Wastewater ~Standard Methods!, 20th ed. (American Public Health Association 1998). In this study, a large-scale direct shear apparatus was built with a length and width of 24 in. ~61 cm! ~Moo-Young et al. 2002!. The shear box measures 12 in. (30.5 cm)! in overall height with the upper and lower portions of the box each measuring 6 in. (15.25 cm). Column tests were conducted using a 12 in. (30.54 cm) diameter by 3 ft (91.44 cm) high PVC column. Physical properties such as specific gravity and water adsorption exhibited no change with increase in shred size. The hydraulic conductivity showed an increase as tire shreds size increased. Laboratory compaction tests were conducted on tire shreds and showed that increasing the compaction energy had little effect on the final compaction density. Direct shear results showed an increase in shear strength as the particle size of tire shreds increases. Also, as the density of the tire shreds increased the shear strength increased. Compression tests showed that as the scrap tire size increased compressibility increased. Thermo Gravimetric Analysis (TGA) tests revealed that tire shreds are stable up to temperatures of 200°C.
M.S. Mashiri (et. Al)	Scrap-tyre soil mixture for seismic protection	The objective of this study was to perform experimental investigation tyre-soil mixtures which involved mixing of scrap tyres with soil materials and place the mixtures around foundation for vibration absorption. Tests on samples were conducted in accordance to Australian standards(AS 1289.5 and AS 1289.2). In Triaxial test, cell pressures used were 69,207,345 and 483 kpa. In sample preparation, mixing of sand and crumbs was carried out manually by stirring both materials with a spoon, producing a homogeneous mixture. The ductility capacity of tyre crumbs and mixture was found to be higher than that of pure sand. Under triaxial test, axial strain at higher confining pressure reflects the ductile behaviour of the mixture. Axial strain in tyre crumb-soil mixture increased with increasing cell pressure and increase in percentage of tyre crumbs. The shear failure envelope of mixtures had a non-linear behaviour. The peak friction decreased with increase in cell pressure.

		The increase in axial strain is linked to ductility of tyre-soil mixture. The gradation of tyre crumbs plays an important role in the strengthening of the soil mixture as failure axial strain may decrease with the increase of the size of tyre crumb.
Hing-Ho Tsang1, S. H. Lo, X. Xu and M. Neaz Sheikh	Seismic isolation for low-to-medium-rise buildings using granulated rubber–soil mixtures: numerical study for Use in Construction rubber–soil mixtures: numerical study	This paper presents the preliminary research works on a potential seismic isolation method that makes use of scrap rubber tires for the protection of low-to-medium-rise buildings. This paper presented a potential GSI system by placing RSM around foundations (raft footing or pile cap) of low-to-medium-rise buildings for reducing seismic demand and exerting a function similar to that of a cushion. It was found that the horizontal acceleration of the roof reduced by 50–70%, horizontal acceleration of the footing by 40–60%, and inter-story drift of the first floor by 40–60%. Also, as the thickness of the RSM increased from 5 to 15m , the percentage (%) reduction in the peak horizontal accelerations of the roof and the footing increased. Also, results showed a higher acceleration reduction for wider (40 and 80m) and lower rise buildings. The use of scrap tires as the rubber material can provide a low-cost and an alternative way of consuming huge stockpiles of scrap tires from all over the world. On average, 40–60% response reduction could be achieved, and the results have been found to be the most sensitive to variations in the thickness of the RSM layer.
A Martelli and M Forni	Seismic isolation of civil buildings in Europe	This review paper outlines the present state of applications of seismic isolation to civil buildings in Europe (with particular reference to Italy), including the countries formerly belonging to the USSR.
M. Neaz Sheikh; M. S. Mashiri; J. S. Vinod; and Hing-Ho Tsang, M.ASCE	Shear and Compressibility Behavior of Sand–Tire Crumb Mixtures	This paper investigates shear and compressibility behaviour of sand–tire crumb (S-TC) mixtures for their application in civil engineering projects. Triaxial and compression tests were conducted on Sand-tire crumb mixtures, where content of tire crumbs varied from 0-40% by volume. It was found that the shear strength of the mixture decreased with increase in content of tire crumb. The peak shear strength and the corresponding axial strain of the mixture increase with the increase in the confining pressure. All mixtures with a percentage of tire crumbs equal to or greater than 10% showed a Brittleness Index (BI) of at least one third of the value of pure sand, indicating a ductile material. The compressibility tests showed that the high compressibility of rubber is inherited in S-TC mixtures, resulting in higher settlements.
Hemanta HAZARIKA, Nobutaka IGARASHI, Yuki YAMADA	Behavior of granular and compressible geomaterial under cyclic loading	The influence of grain size on the material strength and deformation characteristics of granular and compressible materials such as tire chips were evaluated through the static and repetitive direct shear testing as well as the cyclic triaxial testing. Static shear tests were performed at three confining pressures of 100 kPa, 150 kPa, and 200 kPa. Before shearing the test specimens, they were compacted and consolidated for 10 min. Horizontal shearing is then applied at a speed of 0.25 mm/min until displacement reached 50 mm. From the static direct shear testing, it was found that the stress–displacement relation during shearing is highly ductile and exhibits strain hardening. The greater the confining pressure, the higher the development of maximum shear stress. On the other hand, the greater the confining pressures the smaller the difference in the maximum shear strength among the specimens. Cyclic triaxial test results reveal that the cyclic strength of tire chips is strain-dependent
Ali Arefnia,Danial Jahed Armaghani,Ehsan Momeni	Comparative Study on the Effect of Tire-Derived Aggregate on Specific Gravity of Kaolin	The effect of TDA (Tire-Derived Aggregates) on specific gravity of Kaolin is investigated in this paper. The specific gravity test was conducted in accordance with ASTM (D 854-10) standard and Florida test method (FM 5-559). It is observed that specific gravity of kaolin-TDA mixture is increased with any increase in size of TDA while any increase in percentage of TDA would result in a lower specific gravity.

Jorge G. Zornberg, Alexandre R. Cabral, and Chardphoom Viratjandr	Behaviour of tire shred – sand mixtures	In this study, an experimental testing program was undertaken using a large-scale triaxial apparatus with the goal of evaluating the optimum dosage and aspect ratio of tire shreds within granular fills. A large-scale triaxial cell was used in this investigation to test specimens with tire shreds of up to 102 mm (4 in.). Triaxial specimens were prepared with a diameter of 153 mm (6 in.) and a height of 305 mm (12 in.) and tested in a Wykeham Farrance triaxial load frame. The triaxial test results of pure tire shred specimens show an approximately linear deviatoric stress–strain behaviour and a fully contractive volumetric strain behaviour.
G. Venkatappa Rao, Rakesh Kumar Dutta	Compressibility and Strength Behaviour of Sand–tyre Chip Mixtures	This paper investigates to assess the behaviour of the admixtures, compressibility and triaxial compression tests were carried out by varying chip size and chip content. The compressibility and repeated load tests were conducted in a rigid mould having diameter of 15.2 cm and height of 17.8 cm under K0 condition. A standard triaxial apparatus was used for testing sand with and without tyre chips. The tests in a rigid mould (K0 condition) indicate that Vertical strain increases with vertical stress applied, for all chip contents. The variation is significant beyond a stress of 200 kPa and a chip content of 20%. From the drained triaxial test results the following may be concluded the general stress–strain–volume change behaviour of tyre chip–sand mixtures is similar to that of sand. Also, the compressibility becomes excessive for a chip content of more than 20%.
Anbazhagan Panjamani, Hing-Ho Tsang	Earthquake Hazard Mitigation by Utilizing Waste Tires	This paper proposes a new method of utilizing scrap tires for earthquake protection. The method involves mixing scrap tires with soil sediments and placing the mixtures around foundations of building structures for seismic isolation. This paper presented a potential earthquake protection method by placing rubber-soil mixtures (RSM) around foundations (footing or pile) of low-to-medium-rise buildings for absorbing vibration energy and exerting a function similar to that of a cushion.
Sivapalan Gajan and Bruce L. Kutter	Capacity, Settlement, and Energy Dissipation of Shallow Footings Subjected to Rocking	In this paper, several centrifuge experiments were conducted to study the rocking behaviour of shallow footings, supported by sand and clay soil stratums, during slow lateral cyclic loading and dynamic shaking. The testing program includes several series of centrifuge experiments, each of which consists of several shear wall–shallow footing models tested under slow lateral cyclic and dynamic loading conditions. Detailed experimental results are available for all the models tested in the centrifuge in data reports (e.g., Rose brook and Kutter 2001a,b, Gajan et al. 2003; Thomas et al. 2006). Also, it has been shown that the load–displacement behaviour of shallow foundations depends on the applied moment-to-shear ratio at the base of the footing (which is related to the ratio of height of lateral load to length of the footing, h/L). The results presented in this paper show that a rocking footing has very ductile behaviour with negligible loss of capacity, significant energy dissipation capacity, and it includes a self-centring mechanism associated with uplift and gap closure upon unloading.
Sivapalan Gajan and Bruce L. Kutter	Effects of Moment-to-Shear Ratio on Combined Cyclic, Load-Displacement Behaviour of Shallow Foundations from Centrifuge Experiments	This paper presents the findings of a series of centrifuge experiments conducted on shear wall-footing structures supported by dry dense to medium dense sand foundations that are subjected to lateral cyclic loading. Two key parameters, static vertical factor of safety FSV , and the applied normalized moment-to-shear ratio M/ H·L at the footing-soil interface, along with other parameters, were varied systematically and the effects of these parameters on footing-soil system behaviour are presented. As expected, the ratio of moment to the horizontal load affects the relative magnitude of rotational and sliding displacement of the footing. Results also show that, for a FSV, footings with a large moment to shear ratio dissipate considerably more energy through rocking and suffer less permanent settlement than footings with a low moment to shear ratio. The ratio of actual footing area A to the area required to support the vertical and shear loads Ac , called the critical contact area ratio A/Ac , is used to correlate results from tests with different moment to shear ratio. It is found that footings with similar A/Ac display similar relationships between cyclic moment-rotation and cumulative settlement, irrespective of the moment-to-shear ratio. It is suggested that shallow foundations with a sufficiently large A/Ac suffer small permanent settlements and have a well-defined moment capacity; hence they may be used as effective energy dissipation devices that limit loads transmitted to the superstructure.

Mahmoud Ghazavi	Shear strength characteristics of sand-mixed with granular rubber	In the present study, direct shear tests were carried out on rubber particles. The main aim of the tests was to investigate the influence of the particles on shear strength parameters of rubber grain-sand mixtures and also the feasibility of the use of the mixtures as lightweight backfill in geotechnical applications. A relatively, uniform, rounded sand has been chosen. Different contents of waste hose grains have been mixed with the sand at two loose and slightly dense states. The sand alone was tested in direct shear test. The grain size distribution was obtained based on ASTM D422-63 (1989). An average value for the specific gravity of the rubber grains was found to be about 1.13 as tested several times based on ASTM D854-83 (1989). Small direct shear test apparatus with a circular mould having a diameter of 63mm was used to perform shear tests on sand-rubber samples. The thickness of all samples was 20 mm. The tests were carried out based on the procedure described by ASTM D3080-72 (1989). The mixtures contained 10%, 15%, 20%, 50% and 70% waste particles by weight. Two different compaction levels were used. It has been found that an apparent cohesion is obtained in samples containing rubber grains. Furthermore, adding the rubber grains up to 15% to the sand can increase the initial friction of the sand from 37° to 37.6° in more compacted mixtures. In the loose mixtures, varies from 31.2° to 35.3° by adding 15% rubber grains to the sand. The rubber alone had a friction angle of 31°. It was shown that an addition of 10–20% rubber to the sand is optimal to obtain the greatest friction angle. Thus, the shear resistance does not change significantly, however, the rubber grain-sand mixtures are lightweight materials imposing lower lateral earth pressures in retaining structures. Dilation characteristics were observed in sand-rubber mixtures, especially in samples having greater rubber content and more compaction
J. H. Lee, R. Salgado, A. Bernal and C. W. Lovell	Shredded tires and rubber-sand as lightweight backfill	In the present paper, a laboratory study is used for a preliminary assessment of the mechanical properties of tire chips and rubber-sand (a mixture of sand and tire chips or shreds). The results are compared with previous work on similar materials. The properties are then used in the numerical modelling of a full-scale test wall with a tire-shred backfill. Experimental and numerical results are compared. The sand used in the mixtures of tire chips and sand is a commercial sand marketed by U.S. Silica (Ottawa, Ill.) and sold under the trade name Ottawa sand and has been classified under the AASHTO Soil Classification System as A-3. Tire chips with a 30-mm minus size and no exposed steel belting were used to avoid damage to the rubber membranes during the testing program. The sand and tire-chip or tire-shred mixtures will be referred to as rubber-sand. Rubber-sand samples in this study have 40% tire chips by weight. The tri-axial samples were 150 mm in diameter by 300 mm in height. The samples were tested using an MTS Soil Testing System (MTS System Corporation, Eden Prairie, Minn.) connected to a data acquisition system. The tire-chip and rubber-sand samples were compacted using a vibratory method of compaction and tested under consolidated drained conditions. The laboratory test results were used to establish the parameters required for the hyperbolic modelling of these materials. A finite-element analysis was conducted to model the performance of tire-shred and rubber-sand backfills and geotextile reinforced backfills under at-rest and active conditions. The results were compared with field tests performed by Tweedieet al. (1998) at the University of Maine. The finite-element analyses produced reasonably good estimates of deformations and stresses for a tire-shred backfill under at-rest condition, while showing overestimation for the active condition. In addition, the analyses indicated that the performance of rubber-sand, being both lightweight and reasonably strong, compared well with that of a sandy gravel, as a backfill material.
Sompote Youwai and D.T Bergado	Strength and deformation characteristics of shredded rubber tire - Sand mixtures	This paper presents the results of triaxial tests on compacted shredded rubber tire – sand mixtures. The tests were carried out with different mixing ratios of shredded rubber tires and sand. With an increasing proportion of sand in the mixture, the density, unit weight, and shear strength of the mixture increased, but the compressibility decreased. The dilatancy characteristics of shredded rubber tires mixed sand were relatively similar to a cohesionless material and can be explained within a critical state framework. A proposed constitutive model broadly captures the strength and deformation characteristics of a shredded rubber tire – sand mixture at different mixing ratios.
S. Bali Reddy, A. Murali Krishna and Krishna R. Reddy	Sustainable Utilization of Scrap Tire Derived Geomaterials for	This paper provides a review of engineering properties of STD geomaterials and their mixtures with soil (predominantly sand) based on published studies. Further, laboratory model and field studies on typical applications of STD geomaterials/mixtures such as retaining walls, foundations, embankments, and landfills are discussed. Overall, STD

	Geotechnical Applications	geomaterial alone or sand mixed with optimal STD content of 30–40% by weight has been shown to be effective for geoengineering applications.
Il-Sang Ahn, Lijuan Cheng	Tire derived aggregate for retaining wall backfill under earthquake loading	The present research aims at evaluating the dynamic performance of TDA backfill under simulated earthquakes based on a full-scale shake table test. Main test results such as accelerations, wall displacements, and dynamic pressures are presented and discussed in this paper. A comparison with a similar shake table test of a wall with conventional soil backfill shows that the amount of wall sliding increased but the dynamic pressure on the wall exerted by the TDA backfill substantially decreased.
Wei Y. Wu, Christopher C. Benda, and Robert F. Cauley.	Triaxial determination of shear strength of tire chips	Tri axial compression tests following stress paths of constant σ1, were conducted to determine the shear strength of five processed scrap tire products having different gradations and particle shapes according to Standard Specifications for Transportation Materials and Methods of Sampling and Testing (1993). Soil test's autonomous data acquisition unit, Data System 6, was interfaced with an IBM 80286 to record transducer data of displacement and pressures. The inter particle frictional component was separated from the total shear strength according to the energy correction concept proposed by researchers. The experimental results show that all five tire chip products have ultimate inter particle frictional angles of 45° to over 60°. The inter particle frictional component of the strength was fully mobilized and nearly reached a constant value after approximately 5% axial strain. The experimental results confirmed that the strength parameter obtained with constant σ1 was more reasonable. This finding is supported by field observation in which the tire chips have an angle of repose ranging from 37° to 43° (loosely stock piled) and up to 85° (compacted).
Vanessa Cecich, Linda Gonzales, Ase Hoisaeter, Joanne Williams and Krishna Reddy	Use of shredded tires as lightweight backfill material for retaining structures	The purpose of this study is to determine the feasibility of using shredded scrap tires as an alternative backfill material for retaining structures. Laboratory tests were performed in order to obtain the engineering properties of shredded tires. First, sieve analyses were performed using the shredded tire sample both prior to and after compaction in order to determine gradation characteristics. Based on these analyses, the shredded tire sample used for this study was classified as uniform in size, and compaction did not alter the gradation significantly. The unit weight of shredded tires was determined using the modified proctor test set-up, designation D1557 (ASTM 1994),. The permeability of the shredded tires was determined using the constant head permeameter in accordance with ASTM D2434 (ASTM 1994). The shear strength of shredded tires was determined based on the direct shear tests according to ASTM D3080 (ASTM 1994). All of these engineering properties were used for the design of the retaining walls. A detailed geotechnical and structural design of retaining walls was performed for both shredded tires and sand as backfill materials for comparison purposes. To make a thorough comparison, retaining walls were designed for three different heights; 10,20 and 30 ft. A cost estimate was done for each retaining wall and backfill and for a 100-ft wall length. From these estimates, it was determined that using a shredded tire wall instead of a sand wall will generate an average saving of 60%. Based on the results of testing, design and cost analysis, it was to be concluded that using shredded tires as an alternative backfill material is not only economically feasible, but it is also quite economically advantageous. Also, the use of scrap tires as a backfill material helps to reduce the enormous number of tires currently stockpiling in landfills.
S.Bali Reddy ,D . Pradeep Kumar and A Murali Krishna	Evaluation of the Optimum Mixing Ratio of sand tire chips mixture for geo engineering applications	The present study evaluated the Optimum Mixing ratio of STC mixtures for geo engineering applications from the index and mechanical properties of different STC mixtures through laboratory investigations. Specific gravity, density and large size direct shear test were carried out on different STC mixtures
Mahmoud Ghazavi and Masoud Amel Sakhi	Influence of Optimized Tire Shreds on Shear Strength Parameters of Sand.	The influence of dimensions of rectangular shreds prepared from waste tires on the shear resistance of sand shred mixtures has been investigated by performing large direct shear tests. Sand 2,3, &4cm width and various aspect ratios were tested at two different compaction levels. It has been found that shred contents, shred width, shred aspect ratio for given width, compaction and normal stress are influencing factors on shear strength of the mixtures. A number of findings can be citied. dealation characteristics were observed in sand shred mixtures, especially in samples having greater shred content and more compaction. In almost all envelopes Mohr circle is non-linear. The friction angle of mixtures increases by using optimum shred aspect ratio and by increasing shred

		contents and mixture compaction. The tire shreds cause pi to be increased by about 10-94%,depending upon shred width and aspect ratio, shred content and mixture compaction.
Anbazhagan Panjamani	Laboratory Characterization of Tyre Crumbs Soil Mixture for Developing Low cost Damping Materials.	The paper presents maximum and minimum densities, direct shear test and compaction test results for waste materials of tyre crumbs of size 1mm and 2mm mixed with sand and red soil. Study shows that static properties have decreased slightly with increase the tyre crumbs percentage with soil. Further these data may be used in damping scheme by model study, experimental study, vibrating measuring instruments may be used to measure the acceleration or velocity experimentally before and after newly designed isolation scheme.
V.C.Xenaki,G.A.Athanasopoulos	Liquification resistance of sand - silt mixtures;an experimental investigation of the effect of fines.	The liquification resistance of sand-non plastic fines mixtures may either decrease or increase with increasing values of fines content, when compared at the same global void ratio, indicating the existence of a threshold value of fines content. According to the results of the current study the value of FCth is approximately equal to 44%.It should be noted though that the threshold value .FCth, is not unique but it may depend on the characteristics of the coarse and fine grains, as well as on the value of the global void ratio. The conclusion regarding the effect of fines content on the liquefaction resistance of sand-non-plastic fines mixtures drawn upon the effect of fines on the excess pore water pressure generation.
Anbazhagan Pajamani,Manohar Devarahalli Ramegowda and Divyesh Rohit	Low cost damping scheme for low to medium rise buildings using rubber soil mixtures.	This study presents the detailed results of experimental investigation to select the optimum size of tyre crumb from seven crumb sizes. Crumb size F is considered as optimum size based on shear strength, energy absorption capacity and stiffness, compared to other crumb sizes. For the selected crumb size with higher rubber content numerical studies were carried out. Through numerical studies, it was noticed that percentage of rubber in Stickiness and width of RSM around the footing and frequency variation of the input motion are the main factors which controls thr damping characteristics of earthquake motion.
Suat Akbulut,Seracettin Arasan,Ekrem Kalkan	Modification of Clayey Soils using scrap tire rubber and synthetic fibres.	Both lengths and contents of rubber fibres played an important role in the development of UCS of reinforced samples. In general, the UCS values increased with increasing tire rubber fibre contents up to 2% and then decreased. Both the length and the content of synthetic fibres improved the UCS values. The polyethylene and polypropylene fibres increased the UCS values for all contents with maximum at 0.2%.In general, the rubber and synthetic fibres increased the cohesion values. The maximum cohesion values were observed for 10-mm long fibres. The internal friction angle value for each reinforced sample increased in a non-linear way.

CHAPTER 3

3.1 OBJECTIVE

- To check the effect of soil-tire crumb mixture on shear strength and energy absorption capacity of soil
- Its application into vibration isolation
- To find the thickness of Soil-Tire Crumb Mixture layer required for optimum performance

CHAPTER 4

4.1 METHODOLOGY

4.1.1 Site Selection

Site selection was done based on the borehole data. Around 150 borehole data were collected from various civil societies out of those 50 sites were selected based on NSPT values. The site which had NSPT value greater than 35 and sand percentage more than 55% was selected. Based on bore hole data the sites selected were AECS Layout, Kadugodi and Marathahalli.

Table 2 Typical Marathahalli bore hole data

MARATHALLI			
Borehole No	**Soil Type**	**NSPT Value**	**Sand %**
BH 01	Brownish grey silty sand with clay binder	24	41.5
	Brownish grey silty sand with clay binder	35	52.2
BH 02	Brownish yellow clayey sand with gravels	22	51.5
	Brownish yellow clayey sand with gravels	30	56.5

From Table 2 as shown above for the Marathahalli sites, around 4 samples were collected for different sand percentages such as 41.5%, 52%, 51.5% and 56.5%. And these sample were taken into the consideration for our testing.

The same procedure is carried out for Kadugodi and AECS Layout sites using NSPT values and sand percentages to select the sites.

4.1.2 Sampling

Collection of samples i.e. soil in our study is done as per the IS: 2720 codal provisions, taking soil samples at least 1m below the surface to avoid organic content and have a soil

sample at foundation levels. Sites were selected based on the borehole data and the sites having more than 50% of coarse and few other sites too for validating the hypothesis. The basis of this selection was most of the literature had studies on coarse sand mixed with tire crumbs and very less studies on soils. The sites selected were HSR layout, Kadugodi, Marathahalli and Kadubeesanahalli in Bangalore east. 5Kg of samples were collected from each site sealed in a cover to maintain in-situ moisture content. The samples which we collected were disturbed samples and had no homogeneity in them. In-situ density was found out using codal provision of IS: 2720 based on core cutter method and were tabulated.

4.1.3 Materials used

We have used soil samples from different sites and tire crumbs of mixed size for our test. Tire crumbs of mixed size were used because the uniform size tire crumbs when mixed with soil created voids in the soil tire mix and the strength of soil when mixed with uniform size tyre crumbs did not increase appreciably. Hence, buff tire crumbs were used.

4.1.4 Sieve Analysis

IS: 2720 (Part 4) – 1985 – Method of test for soil (Part 4-Grain size analysis). Sieve analysis apparatus is shown in Fig. 8.

Fig. 8 Sieve Analysis Apparatus

Equipment & Apparatus:

- Balance
- Sieves

- Sieve shaker

Preparation of sample: After receiving the soil sample, it is dried in air or in oven (maintained at a temperature of 600C). If clods are there in soil sample, then it is broken with the help of wooden mallet.

4.1.4.1 Procedure:

1. The sample is dried to constant mass in the oven at a temperature of 1100±50C and all the sieves which are to be used in the analysis are cleaned.

2. The oven dry sample is weighed and sieved successively on the appropriate sieves starting with largest. Each sieve is shaken for a period of not less than 2 minutes.

3. On completion of sieving the material retained on each sieve is weighed.

4.1.4.2 Calculation:

1. The percent retained (%), Cumulative retained (%) & percent finer (%) is calculated.
2. Percent retained on each sieve = Weight of retained sample in each sieve / Total weight of sample
3. The cumulative percent retained is calculated by adding percent retained on each sieve as a cumulative procedure.
4. The percent finer is calculated by subtracting the cumulative percent retained from 100 percent.
5. D50 of the soil is then determined from the gradation curve.

4.1.5 Standard Proctor Compaction

Compaction is a method of mechanically increasing the density of soil, and it's especially valuable in construction applications. If this process is not performed properly, soil settlement can occur, resulting in unnecessary maintenance cost or failure of the pavement or structure. By compacting the soil, load capacity and stability increases, the permeability decreases, the water seepage reduces, compaction prevents settlement of the soils or damage from frost

We have done standard proctor compaction test on every sample to get the optimum moisture content for that sample.

4.1.5.1 Procedure

1. 5 kg oven dried sample was taken in the pan. 4-6% water was added and mixed thoroughly.
2. The proctor mould without base plate and collar was weighed. The base plate and the collar were fixed.
3. The sample was filled in 3 layers and given 25 blows in each layer with a rammer of 2.5kg.
4. The collar was removed, and compacted soil was trimmed to the top of mould.
5. The weight of compacted specimen was divided by the volume of the mould and bulk density was calculated.
6. Break the specimen as it should pass 4.75mm sieve. water in enough amounts is added to increase the moisture content of soil sample by one or two percentage.
7. The above procedure for each increment of water is repeated and it is continued until there is decrease or no change in wet unit weight of compacted soil.

4.1.6 Sample preparation

Sample preparation refers to the ways in which a sample is treated prior to its analysis. Preparation is a very important step in most analytical techniques, because the techniques are often not responsive to the analyte in its in-situ form, or the results are destroyed by interfering species. Different samples were prepared for the direct shear and UU triaxial test that is to be done.

4.1.7 Direct Shear Test - Sample preparation

IS: 2720(Part 13)-1986- Methods of test for soils: Direct shear test.

4.1.7.1 Equipment / apparatus:

- Shear box
- Box container
- Porous stone and grid plate
- Tamper, Balance, Sieve (4.75 mm)
- Loading frame, Proving ring, Dial

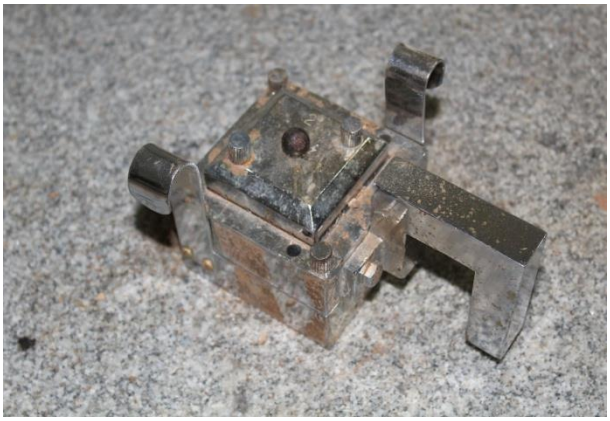

Fig. 9 Shear box

4.1.7.2 Preparation of sample:

One kg of air-dry sample passing through 4.75mm IS sieve is required for this test. Shear box is shown in Fig. 9.

4.1.7.3 Procedure:

1. Shear box dimensions is measured, the box is set up by fixing its upper part to the lower part with clamping screws, and then a porous stone is placed at the base.

2. For undrained tests, a serrated grid plate is placed on the porous stone with the serrations at right angle to the direction of shear. For drained tests, a perforated grid is used over the porous stone.

3. An initial amount of soil is weighed in a pan. The soil is placed into the shear box in three layers and for each layer is compacted with a tamper. The upper grid plate, porous stone and loading pad is placed in sequence on the soil specimen.

4. The pan is weighed again, and the mass of soil used is computed.

5. The box is placed inside its container and is mounted on the loading frame. Upper half of the box is brought in contact with the horizontal proving ring assembly. The container is filled with water if soil is to be saturated.

6. The clamping screws is removed from the box and set vertical displacement gauge and proving ring gauge to zero.

7. The vertical normal stress is set to a predetermined value. For drained tests, the soil is allowed to consolidate fully under this normal load. (Avoid this step for undrained tests.)

8. The motor is started with a selected speed and shear load is applied at a constant rate of strain. Readings of the gauges are taken until the horizontal shear load peaks and then falls, or the horizontal displacement reaches 20% of the specimen length.

9. The moisture content of the specimen is determined after the test. The test is repeated on identical specimens under different normal stress values.

4.1.7.4 Calculation:

- The density of the soil specimen is calculated from the mass of soil and the volume of the shear box.
- The dial readings are converted to the appropriate displacement and load units by multiplying with respective least counts.
- Shear strains are calculated by dividing horizontal displacements with the specimen length, and shear stresses are obtained by dividing horizontal shear forces with the shear area.
- The shear stress versus horizontal displacement is plotted. The maximum value of shear stress is read if failure has occurred, otherwise read the shear stress at 20% shear strain. The maximum shear stress versus the corresponding normal stress is plotted for each test, the cohesion and the angle of shearing resistance of the soil is determined from the graph.

4.1.8 UU Triaxial Test sample preparation

In order to prepare the pat, we found the OMC of different soil using standard proctor test. The OMC of different soils is shown in the Table 3. The following procedure is carried out for the preparation of pat.

1) For 0% Pat 300g of soil and 0g of tyre crumbs were mixed together. Water corresponding to the amount of OMC of the respective site was used.
2) For 0% Pat 292.5g of soil and 7.5g of tyre crumbs were mixed together. Water corresponding to the amount of OMC of the respective site was used.

3) For 0% Pat 285g of soil and 15g of tyre crumbs were mixed together. Water corresponding to the amount of OMC of the respective site was used.

Table 3 OMC and Density of soils used

Sample No.	Soil	OMC	Density (kN/m^3)
1	A Block AECS Layout	16%	21.68
2	Kadugodi	17%	18.64
3	M.K Retail	15%	21.09
4	Ragham	16%	15.79
5	Ramdev	26%	17.25

4) For 0% Pat 277.5g of soil and 22.5g of tyre crumbs were mixed together. Water corresponding to the amount of OMC of the respective site was used.
5) For 0% Pat 270g of soil and 30g of tyre crumbs were mixed together. Water corresponding to the amount of OMC of the respective site was used.

UU Triaxial pat and test apparatus is shown in Fig. 10 and Fig. 11 respectively.

Fig. 10 UU Triaxial pat

Fig. 11 Triaxial Test Apparatus

4.1.8.1 Procedure

Triaxial test are one of the most widely performed tests in a geotechnical laboratory the advantage of the test over other test methods used in the geotechnical laboratory used to determine shear strength is that specimen drainage can be controlled, and pore pressure can be measured. The triaxial test enables parameters such as cohesion, internal angle of friction and shear strength to be determined.

1) The pat is placed between two porous stones.
2) A rubber membrane is then wrapped over the pat.
3) Four O-rings are fit over the membrane. The whole setup is placed into the UU Triaxial apparatus.
4) The water is filled in the setup until it escapes from the bleed valve, which is then closed.
5) The cell pressure of 50kpa, 100kpa and 200kpa are applied without allowing drainage.
6) Deviator stress is then applied keeping cell pressure constant without allowing drainage.
7) The proving ring reading is noted at interval of 25 dial gauge reading until failure.
8) Stress and strain are calculated using proving ring reading and dial gauge reading.
9) The graph is plotted between deviatoric stress and strain.

The area under the stress-strain curve up to a given value of strain is the total mechanical energy per unit volume which the material consumed while straining it to that value (Roylance, 2001). This is given by:

$$EA = \int_0^{\epsilon} \sigma(\epsilon) d\epsilon \qquad (1)$$

where $\sigma(\epsilon)$ is stress as a function of strain. The Energy Absorption (EA) capacity (toughness) of the mix is determined by the area under the stress-strain curve obtained from

UU triaxial tests. The area up to the yield point is the modulus of resilience and the total area up to fracture is the modulus of toughness. Ductility can be determined by the brittleness index based on the equation defined by Bishop (1967), which has been used in recent journals (Fatahi et al., (2015); Anbazhagan et al., (2015)):

$$I_B = \frac{qf-qu}{qu} \qquad (2)$$

Where q_f and q_u are the peak deviatoric stress and the residual deviatoric stress respectively. As brittleness index approaches zero, failure mechanism becomes more ductile.

4.1.9 DEEPSOIL (Analysis Software)

DEEPSOIL has been under development at UIUC since 1998. The driving motivation of the development of DEEPSOIL was and continues to be making site response analysis readily accessible to students, researchers and engineers worldwide and to support research activities at UIUC. In DEEPSOIL we maintain that it is always necessary to perform equivalent linear (EL) in conjunction with nonlinear (NL) site response analyses. Therefore, DEEPSOIL, since its inception, has incorporated both analysis capabilities. Version 6 of DEEPSOIL gives the user the option to automatically obtain EL analysis results whenever an NL analysis is selected without the need to separately develop an EL profile. DEEPSOIL v6.1: The GQ/H nonlinear model is added to DEEPSOIL allowing the user to specify soil strength in a Generalized Hyperbolic Model.

4.1.9.1 Program Organization

The DEEPSOIL graphical user interface is composed of several steps to guide the user throughout the site response analysis process as illustrated in the Navigation box shown in Figure 8 presented to the user upon starting DEEPSOIL.

At the top left, the user has the option of choosing the “Analysis,” “Motions,” or “Profiles” tab. These tabs are discussed in the following section.

Figure 12 and 13 show the main window and key tables. The Options window can be accessed by clicking on the “Options” menu. The window allows the user to set the default

working directory, the directory containing input motions for use in analyses, the default directory in which to save profiles, the default units, the analysis priority, and enable or disable multi-core support.

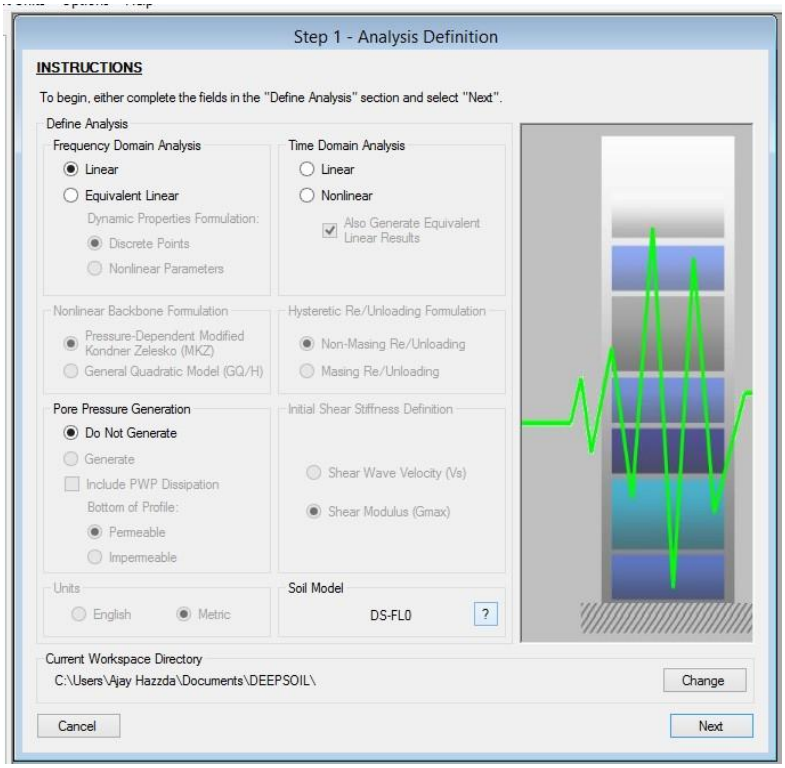

Fig. 12 DEEPSOIL First Window and Key Tabs

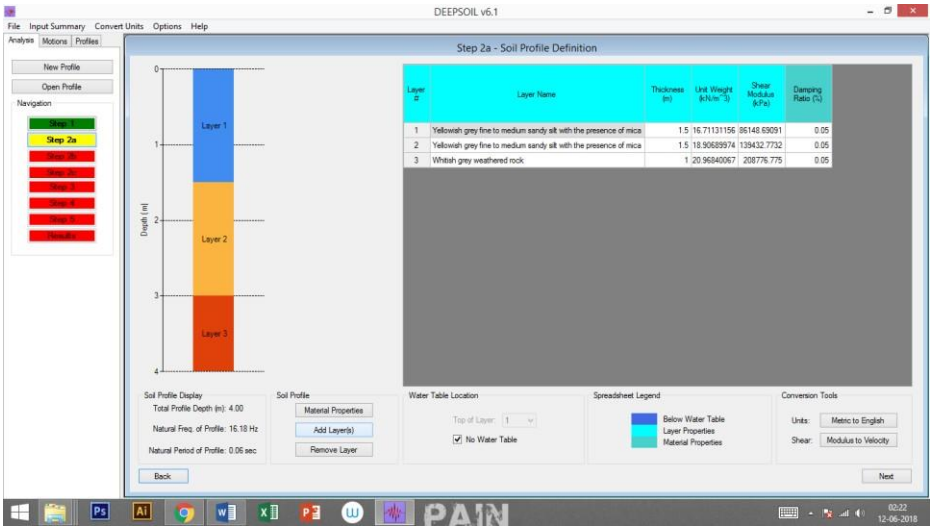

Fig. 13 DEEPSOIL Main Window

4.1.9.2 Motions Tab

DEEPSOIL contains a motion tab which can be used to view/process input motions. To view/process a motion, simply select it from the list and press the View button. A new window will open and DEEPSOIL will generate acceleration, velocity, and displacement and Arias intensity time histories, as well as the response spectrum and Fourier amplitude spectrum for the selected motion. The relative size of the plots can be adjusted by clicking on the gray vertical line and dragging to the left or right. Double-clicking on the response spectrum and Fourier amplitude spectrum plots will cause the axes to alternate between linear and log scales on the axes (each plot supports 3 different views). The calculated data is also provided for the user in data tables which can be accessed by selecting the "Time History Data" or "Spectral Data" tabs at the top of the window. Motion viewers Plots and Tables are shown in Fig. 14 and Fig. 15.

This window also provides the user the option to linearly scale the selected input motion. The user is provided two options for scaling: scale the original motion by a specified factor (scale by) or scale the original motion to a specified maximum acceleration (scale to). The desired method can be selected using the drop-down list in the upper right corner of the window. Press the Apply button to scale the motion and recalculate the other data. After scaling, the user can save the new motion by pressing the Save As button.

4.1.9.3 Response Spectra Calculation Methods

The frequency-domain solution, the New mark β method and Duhamel integral solutions are the three most common methods employed to estimate the response of Single Degree of Freedom (SDOF) systems and therefore to calculate the response spectra. A brief description is presented for each method to calculate the response of SDOF systems is presented for each method to calculate the response of SDOF systems.

Frequency-domain solution in the frequency-domain solution, the Fourier Amplitude Spectra (FAS) input motion is modified by a transfer function defined as:

$$H(f) = \frac{-f_n^2}{(f^2 - f_n^2) - 2i\xi f f_n} \quad (3)$$

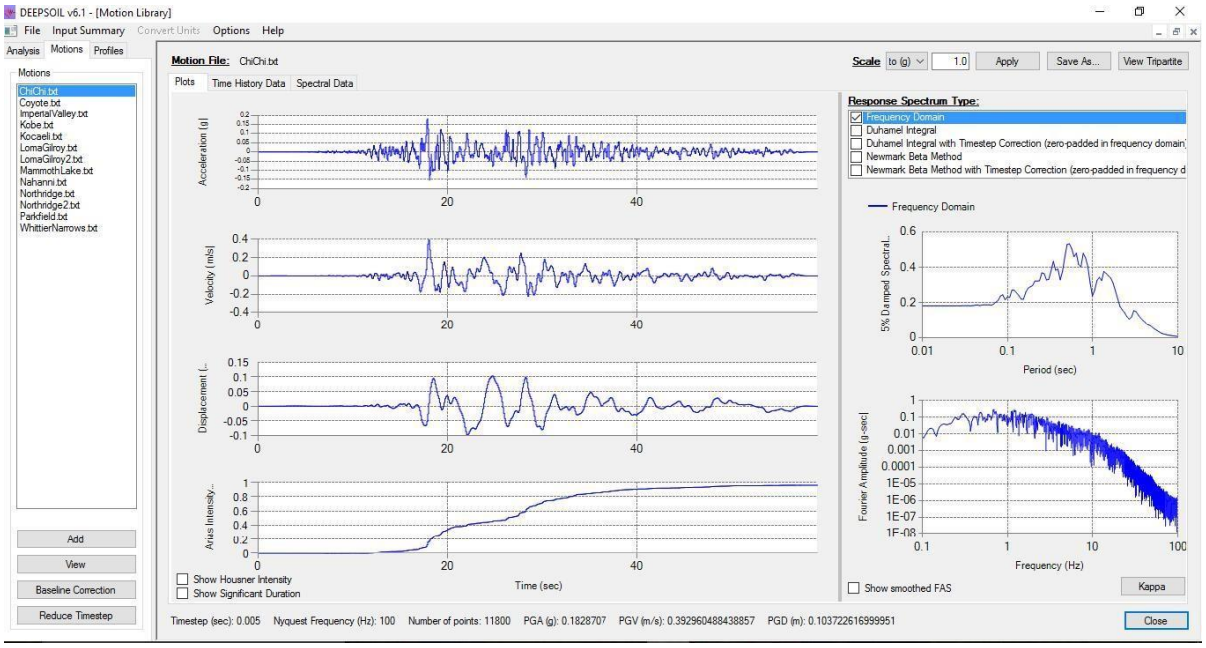

Fig. 14 Motion Viewers (Plots)

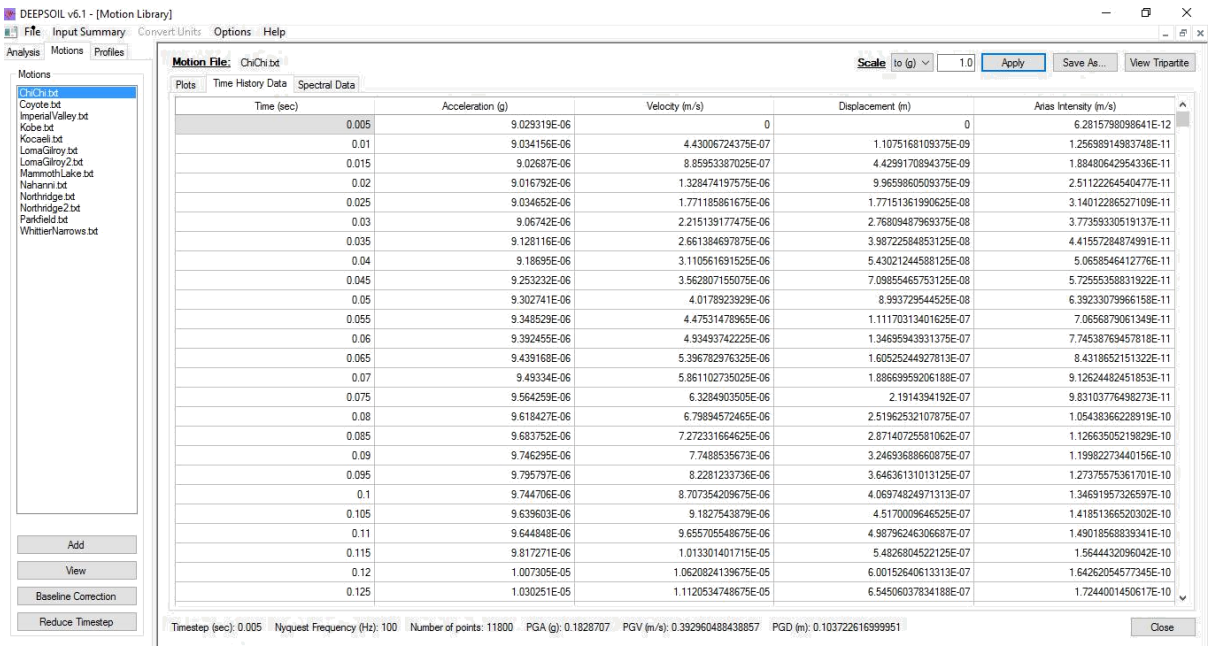

Fig. 15 Motion Viewers (Tables)

4.1.9.4 Analysis Flow

To create a new analysis, the user must specify the type of analysis before proceeding to the next stage of analysis. The user must specify:

1. The analysis method:
   - Frequency Domain
     - Linear
   - Equivalent Linear
     - Time Domain
     - Linear
     - Nonlinear
2. The type of input for shear properties:
   - Shear Modulus
   - Shear Wave Velocity
3. The units to be used in analysis:
   - English
   - Metric
4. The pore water pressure control:
   - No pore water pressure generation
   - Pore water pressure generation without dissipation (nonlinear only)
   - Pore water pressure generation and dissipation (nonlinear only)
5. The method to define the soil curve:
   - For Equivalent Linear
     - Discrete Points
     - Any model supported for nonlinear analyses

- For Nonlinear
    - MRDF Pressure-Dependent Hyperbolic Model
    - Pressure-Dependent Hyperbolic Model
    - MRDF General Quadratic/Hyperbolic Model
    - General Quadratic/Hyperbolic Model

6. The pore water pressure boundary condition at the bottom of the soil profile (for analysis with PWP generation and dissipation)

- Permeable
- Impermeable

After selecting they type of analysis, the Soil Model description will be updated. These identifiers are included in the analysis results file and can be used to quickly convey the type of analysis that was performed. The soil model identifiers are shown in Fig. 16.

Model	Description
DS-FL0	Frequency Domain Linear
DS-EL0	Frequency Domain Equivalent Linear - Discrete Points
DS-EL1	Frequency Domain Equivalent Linear - MKZ with Masing Rules
DS-EL2	Frequency Domain Equivalent Linear - MKZ with Non-Masing Behavior
DS-EL3	Frequency Domain Equivalent Linear - GQ/H with Masing Rules
DS-EL4	Frequency Domain Equivalent Linear - GQ/H with Non-Masing Behavior
DS-TL0	Time Domain Linear
DS-NL1	Time Domain Nonlinear - MKZ with Masing Rules
DS-NL2	Time Domain Nonlinear - MKZ with Non-Masing Behavior
DS-NL3	Time Domain Nonlinear - GQ/H with Masing Rules
DS-NL4	Time Domain Nonlinear - GQ/H with Non-Masing Behavior
-PWP0	Porewater pressure generation without dissipation
-PWP1	Porewater pressure generation and dissipation - permeable halfspace
-PWP2	Porewater pressure generation and dissipation - impermeable halfspace

Fig. 16 Soil Model Identifiers in DEEPSOIL

4.1.9.5 Equivalent Linear Analysis

The equivalent linear model employs an iterative procedure in the selection of the shear modulus and damping ratio soil properties as pioneered in program SHAKE. These properties can be defined by discrete points or by defining the soil parameters that define the backbone curve of one of the nonlinear models.

The option of defining the soil curves using discrete points is only applicable for the Equivalent Linear analysis. For this option, the G/Gmax and damping ratio (%) are defined as functions of shear strain (%).

4.1.9.6 Deconvolution via Frequency Domain Analysis

This approach is the same as the frequency-domain linear equivalent linear analysis approaches except that the input motion can be applied at the ground surface or anywhere else in the soil column. The corresponding rock motion is then computed and provided to the user.

Deconvolution requires definition of a soil profile. The following properties need to be defined for each layer:

- Thickness
- Shear Wave Velocity (m/s) or Initial Shear Modulus (N/sq.mm)
- Damping Ratio (%)
- Unit Weight

To perform the deconvolution,

1. Open or create a frequency domain profile.
2. Enter the requested information into the table on Step 2a,
3. Additional layers may be added using the Add Layer button. Unwanted layers may similarly be removed using the Remove Layer button.
4. Click Next to advance through Steps 2b to Step 2c.
5. On Step 2c, check the box labelled Deconvolution near the bottom of the window.

6. Specify the point of application of the ground motion by selecting the appropriate layer in the drop-down list.

7. Use the circular buttons to select the type of ground motions for generated as output.

8. Click Next to advance to Step 3 and select the locations for output and the motion(s) to be deconvolved.

9. Click Next to advance to Step 5 and set the frequency-domain parameters.

10. Click Analyze.

4.1.9.7 Output from DEEPSOIL:

Upon completion of analysis, the following output for each selected layer will be directly exported to a text file “Results - motion.txt” in the working directory specified in step 1.

For “Total Stress Analysis”

- Acceleration (g) vs Time (sec)
- Strain (%) vs Time (sec)
- Stress (shear/effective vertical) vs Time (sec)
- Response Spectra: PSA (g) vs Period (sec)
- Fourier Amplitude (g-sec) vs Frequency (Hz)
- Fourier Amplitude Ratio (surface/input) vs Frequency (Hz)
- PGA Profile: Max PGA vs Depth
- Strain Profile: Max Strain vs Depth

For “Effective Stress Analysis”

- All from “Total Stress Analysis”

- Pore Water Pressure (pwp/effective vertical) vs Time (sec)
- PWP Profile: Max PWP Ratio vs Depth

If multiple motions were selected for analysis, the output can be found in the user's working directory in a folder named "Batch Output". Within this folder, there will be a folder corresponding to each collection of batch analyses (i.e. Batch0, Batch1, etc.). These folders will contain the results from each motion.

If a single motion was selected for analysis, the results can be found in the user's working directory. After analysis is complete, the user may immediately view the following output visually by selecting the appropriate tab for the selected layer:

- Acceleration (g) vs Time (sec)
- Velocity (ft/sec or m/sec) vs Time (sec)
- Relative Displacement (ft or m) vs Time (sec)
- Arias Intensity (ft/sec or m/sec) vs Time (sec)
- Strain (%) vs Time (sec)
- Stress (shear/effective vertical) vs Time (sec)
- Stress (shear/effective vertical) vs Strain (%)
- Excess Pore water Pressure (excess/effective vertical) vs Time (sec) (if applicable)
- Fourier Amplitude (g-sec) vs Frequency (Hz)
- Fourier Amplitude Ratio (surface/input) vs Frequency (Hz)
- Response Spectra: PSA (g) vs Period (sec)

4.1.9.8 Output data file

Output data for each layer analyzed is automatically exported to “Results – motion.txt” in the user’s working directory. DEEPSOIL also provides the option to export the analysis results to a Microsoft Excel file.

4.1.9.9 Summary Profiles

Shown in Fig. 17, the Summary Profiles Window shows the PGA, maximum strain, and maximum shear stress ratio for each layer. If an analysis with pore water pressure generation was conducted, this window will also show the maximum excess pore water pressure ratio (excess/effective vertical) for each layer. Note that the PGA is calculated at the top of each layer, while all other values are calculated at the midpoint of each layer. To view the layers in the plots, check Show Layers. To change the color of the plotted layer lines, click the color box and select a new color. When you are finished, press Back to return to the output plots.

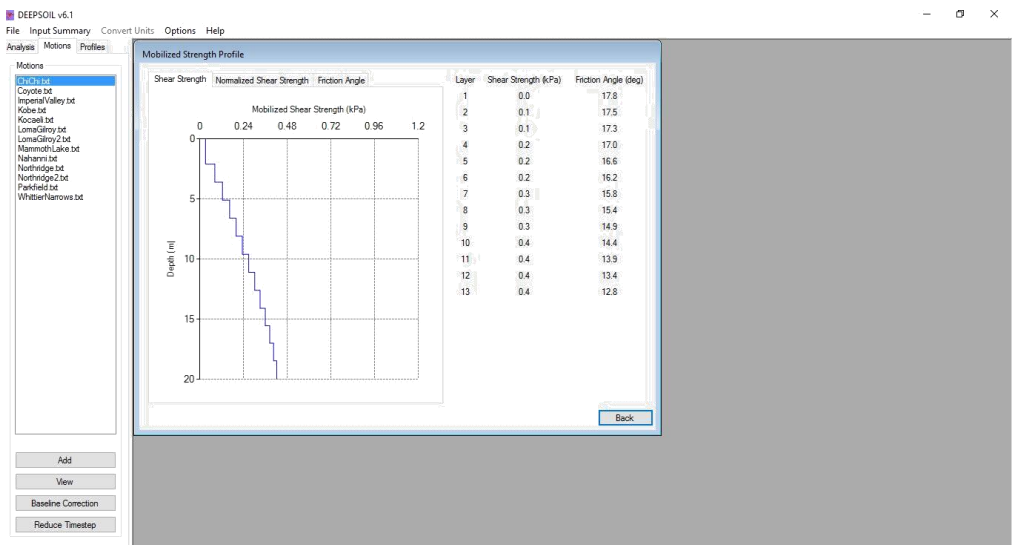

Fig. 17 Summary Profile

4.1.9.10 Displacement Profile and Animation

The Column Displacement Animation Window allows the user to adjust the speed of the animation as well as to stop the animation and show the displacement at a given time. These options can be adjusted using the scroll bars below the plot. Click Start to start the animation or click Back to return to the output plots. The shear strength profile, response

spectra summary and column displacement is shown in Fig. 18, Fig. 19 and Fig. 20 respectively.

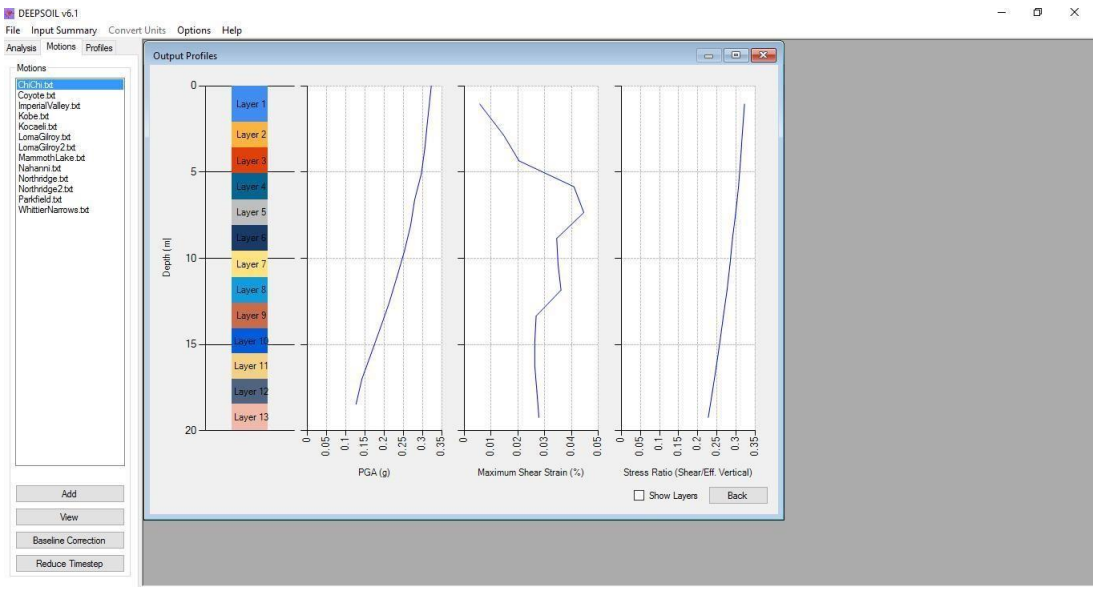

Fig. 18 Shear Strength Profile

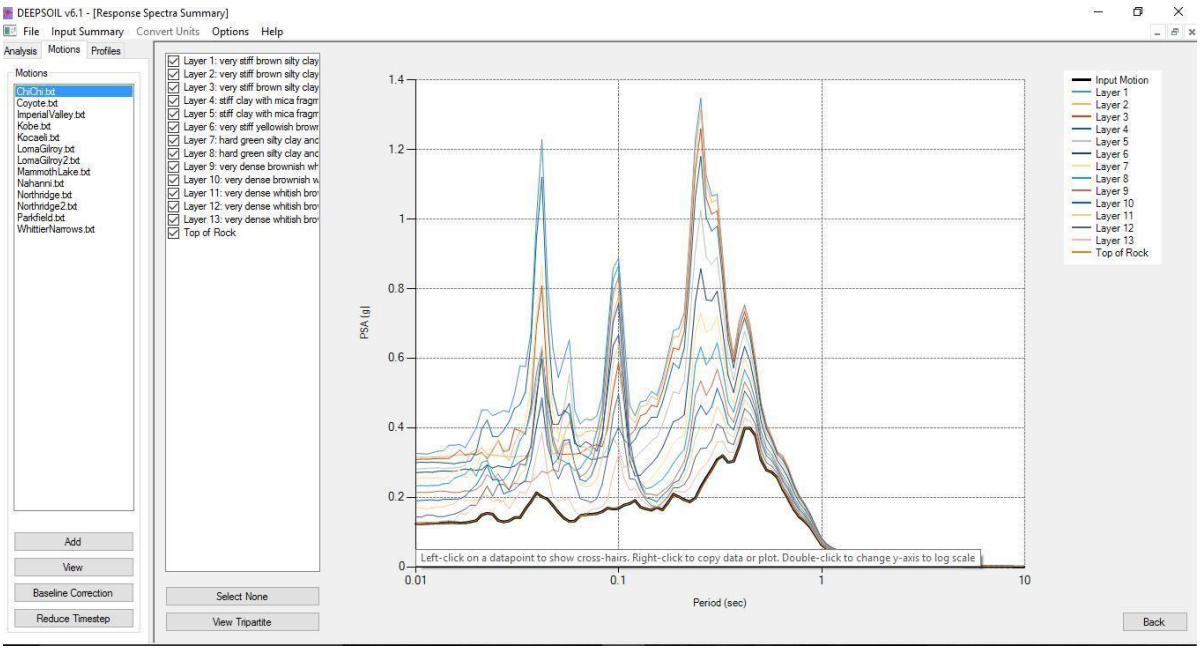

Fig. 19 Response Spectra Summary

Effective stress

Ground movements and instabilities can be caused by changes in total stress (such as loading due to foundations or unloading due to excavations), but they can also be caused by changes in pore pressures (slopes can fail after rainfall increases the pore pressures).

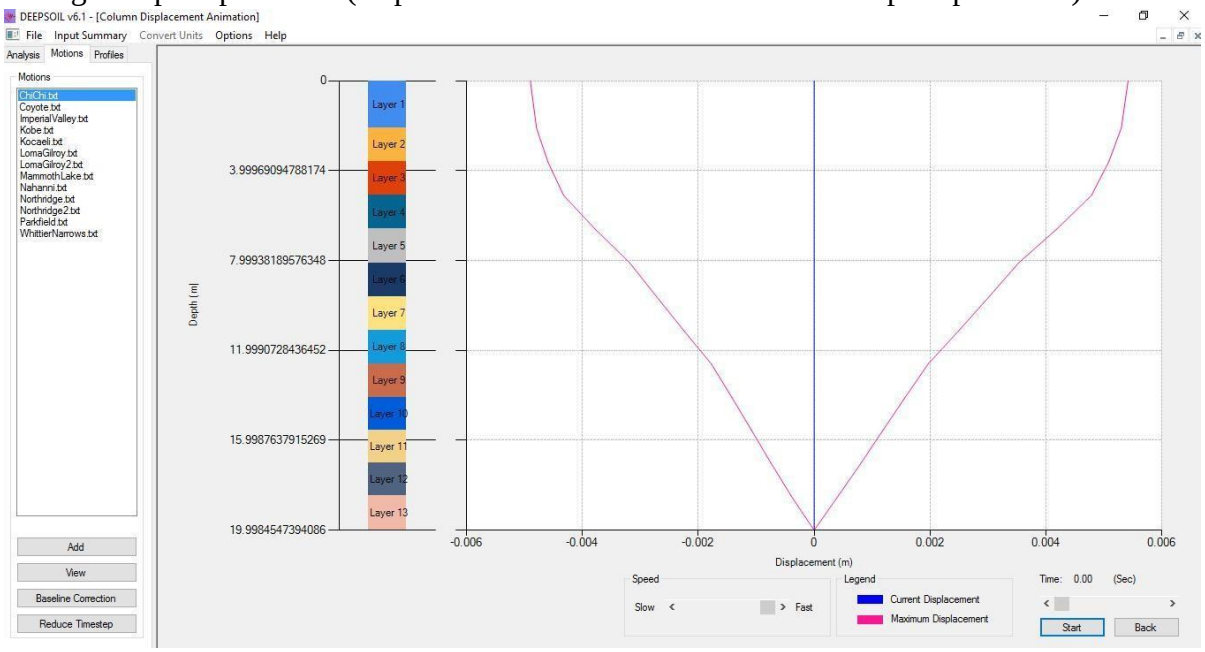

Fig. 20 Column Displacement

In fact, it is the combined effect of total stress and pore pressure that controls soil behaviour such as shear strength, compression and distortion. The difference between the total stress and the pore pressure is called the effective stress:

Effective stress = Total stress - Pore pressure

or $\sigma' = \sigma - u$

Stress Ratio

Stress ratio in DEEPSOIL is the ratio of shear stress to effective vertical stress. It is desirable that the stress ratio is higher which indicates the reduction of effective vertical stress. This is desirable because as when the effective vertical stress decreases, the impact of input motion is reduced.

Input Motion

The input motion given to the elastic half space is Koyna earthquake, which had occurred at Koynanagar, Maharashtra on December 11, 1967. The magnitude 6.6 shock hit with a

maximum Mercalli intensity of VIII. This earthquake in Deccan Plateau had an intensity which has an occurrence period of 100 years. Hence, two versions of this earthquake were used for analysis – one which was not scaled down and the other which was scaled down, which would have an occurrence period of 30 years, which would probably occur in a lifespan of a building. The PGA of the input motions used are 0.36g and 0.1g respectively. Hence, a high intensity strong ground motion and a low intensity ground motion are used as input motions.

CHAPTER 5

RESULTS AND DISCUSSION

Sieve analysis was done on soil samples to obtain its grain size distribution and its D50 value. Shear strength, energy absorption and deformation characteristics of the composite materials were examined with respect to the size of tire crumbs, the percentage of tire crumbs and the applied normal stress on the samples in direct shear and UU triaxial test. Here, the results of the laboratory tests are presented with discussion highlighting the effects of various parameters.

5.1 SIEVE ANALYSIS

Sieve analysis was done on every soil sample to obtain its grain size distribution and D50 value. Figure 21 shows the grain size distribution curve of Site 1, Site 2 and Site 3 soil samples. The values of Uniformity Coefficient (Cu) and Coefficient of Curvature (Cc) for Site 1 soil sample were found to be 5.59 and 1 respectively, stating the soil to be well-graded. The D50 value for this soil sample was found to be 0.79, stating the soil to be medium-grained. With D50 value of the soil being 0.79, the coarse content of the soil was found to be 51.26%.

The values of Uniformity Coefficient (Cu) and Coefficient of Curvature (Cc) for Site 2 soil sample were found to be 7.12 and 0.66 respectively. The D50 value for this soil sample was found to be 1, stating the soil to be medium-grained. With D50 value of the soil being 1, the coarse content of the soil was found to be 51.28%. The values of Uniformity Coefficient (Cu) and Coefficient of Curvature (Cc) for Site 3 soil sample were found to be 5.39 and 0.96 respectively. The D50 value for this soil sample was found to be 0.71, stating the soil to be medium-grained. With D50 value of the soil being 0.71, the coarse content of the soil was found to be 51.82%. The D50 values for Soil samples 4 and 5 were found to be 1.4 and 0.95 respectively.

5.2 DIRECT SHEAR TEST

Figure 22 shows the variation of shear stress with normal pressures for various percentages of tire crumbs on Site 1 soil sample. The influence of tire crumb content can be observed

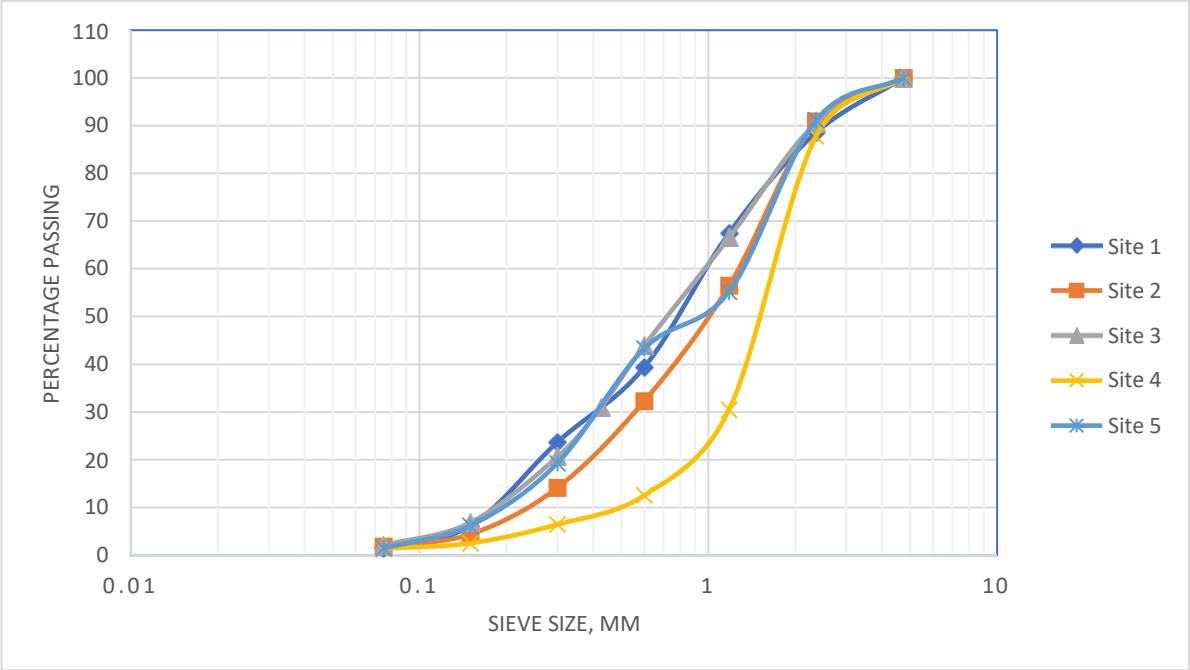

Figure 21 Grain size distribution curves for Site 1,2 and 3 soil samples

by the significant increase in the shear stress value, especially when the percentage of tire crumbs was 2.5% and 5%. A steady increase in shear strength was observed for increasing normal pressure with increase in tire crumbs percentage. The increase in strength follows a similar trendline as pure soil at initial tire crumb percentages. As the percentage of tire crumbs increased, an initial increase in strength was observed at lower normal pressures but at high normal pressure, there was a substantial decrease in shear strength.

The variation of shear stress with normal pressures for various percentages of tire crumbs on Site 2 soil sample is shown in Figure 23. For this soil sample, a steady increase in shear strength was observed for increasing normal pressure with increase in tire crumbs percentage. The variation of shear stress with respect to normal pressure for increasing tire crumbs percentage followed a similar trendline compared to pure soil variation. While there was a very slight decrease in shear stress at higher tire crumbs percentage at lower normal pressures, the increase in shear strength with increase in normal pressure was more predominant.

Figure 24 shows the variation of shear stress with normal pressures for various percentages of tire crumbs on Site 3 soil sample. Here, there is a general decrease in shear strength when

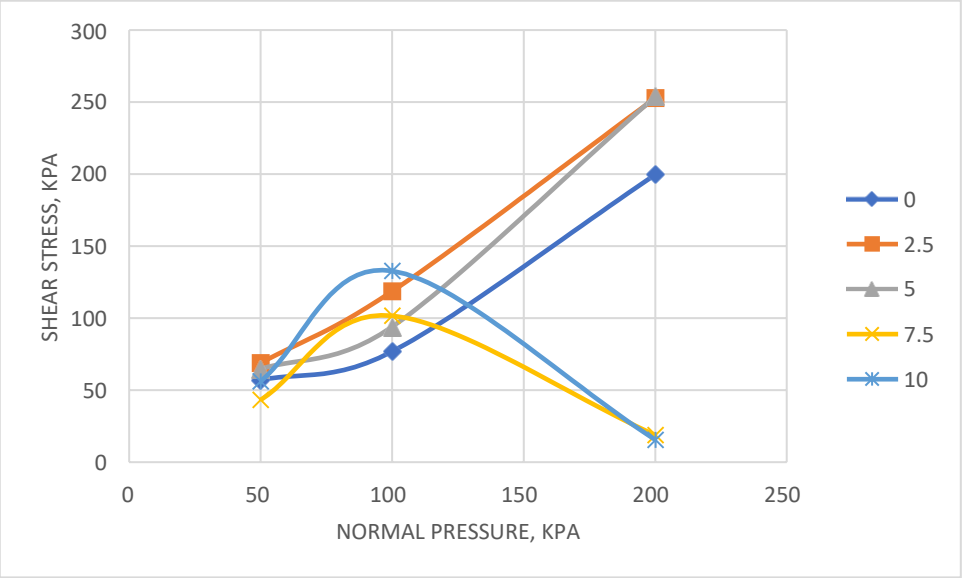

Figure 22 Variation of Stress vs Normal Pressures for different percentages of tire crumbs for Site 1 Soil Sample

compared to shear strength of pure soil for initial confining pressures for all percentages of tire crumbs. But this is followed by a general increase in shear strength for all percentages of tire crumbs. This increase in strength is higher compared to other tire crumb percentages when the tire crumbs percentage is 10%.

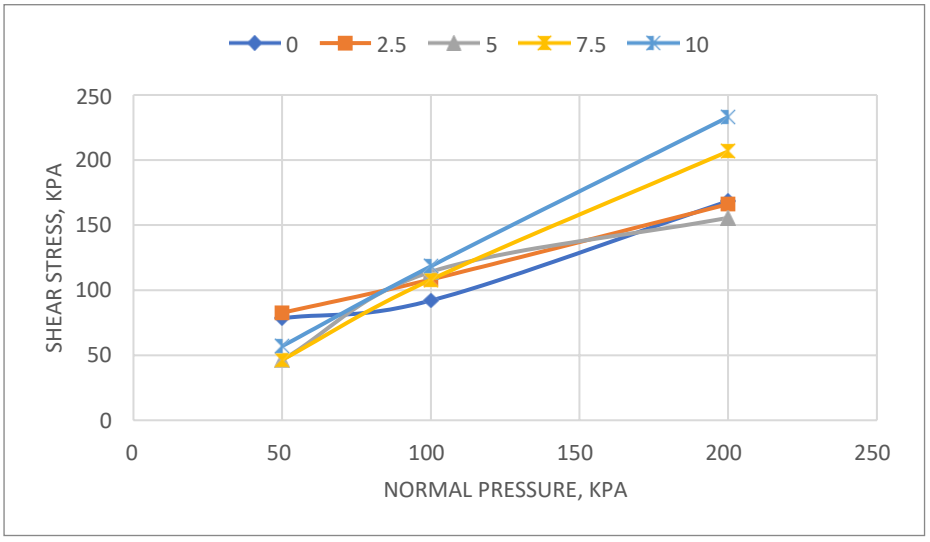

Figure 23 Variation of Stress vs Normal Pressures for different percentages of tire crumbs for Site 2 Soil Sample

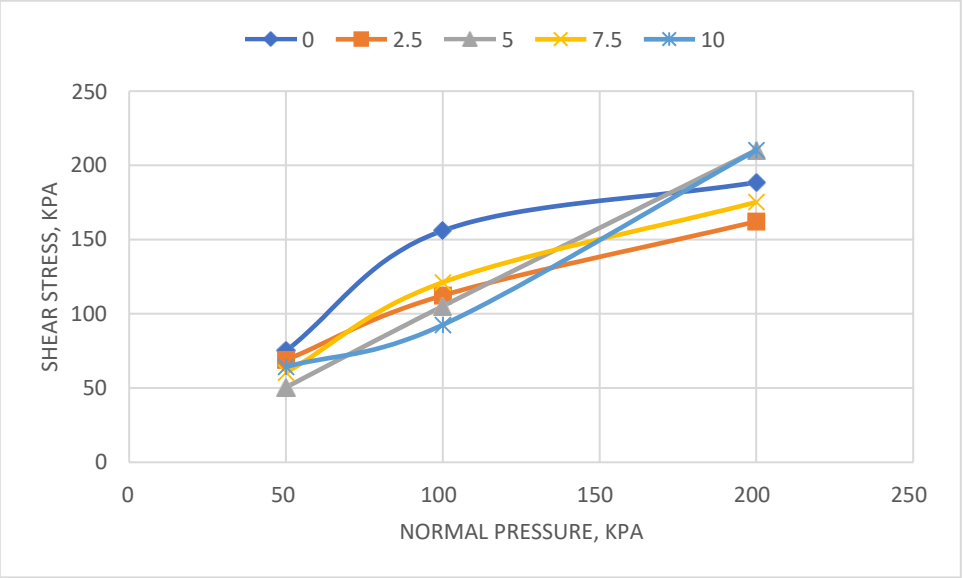

Figure 24 Variation of Stress vs Normal Pressures for different percentages of tire crumbs for Site 3 Soil Sample

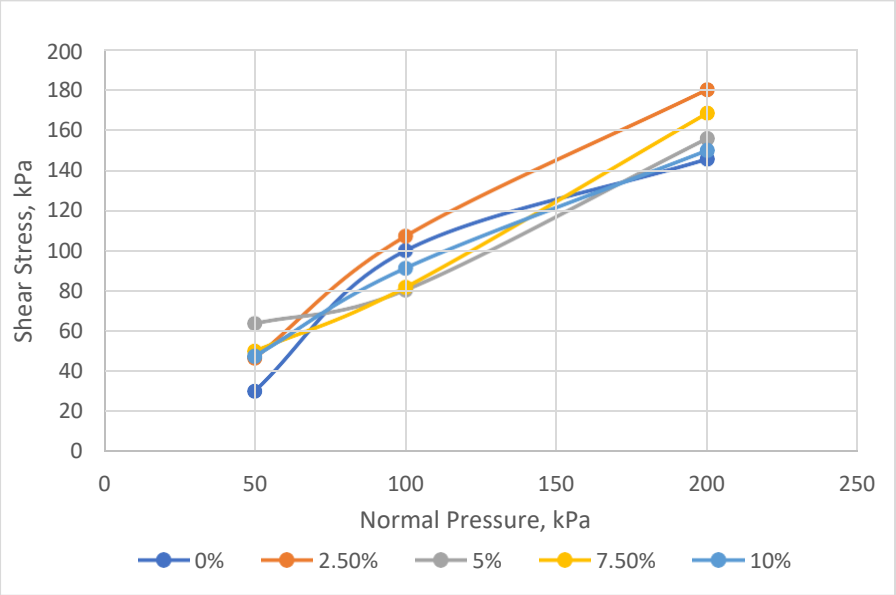

Figure 25 Variation of Stress vs Normal Pressures for different percentages of tire crumbs for Site 4 Soil Sample

Figure 25 shows the variation of shear stress with normal pressures for various percentages of tire crumbs on Site 4 soil sample. Here, there is a general decrease in shear strength when compared to shear strength of pure soil for initial confining pressures for all percentages of

tire crumbs other than 2.5%. But this is followed by a general increase in shear strength for all percentages of tire crumbs at higher confining pressures. This increase in strength is higher compared to other tire crumb percentages when the tire crumbs percentage is 2.5%.

Figure 26 shows the variation of shear stress with normal pressures for various percentages of tire crumbs on Site 5 soil sample. The influence of tire crumb content can be observed by the increase in the shear stress value, especially when the percentage of tire crumbs was 2.5% and 5%. A steady increase in shear strength was observed for increasing normal pressure with increase in tire crumbs percentage. The increase in strength follows a similar trendline as pure soil at initial tire crumb percentages. As the percentage of tire crumbs increased, an initial increase in strength was observed at lower normal pressures but at high normal pressure, there was a substantial decrease in shear strength except at 2.5% and 5% tire crumbs.

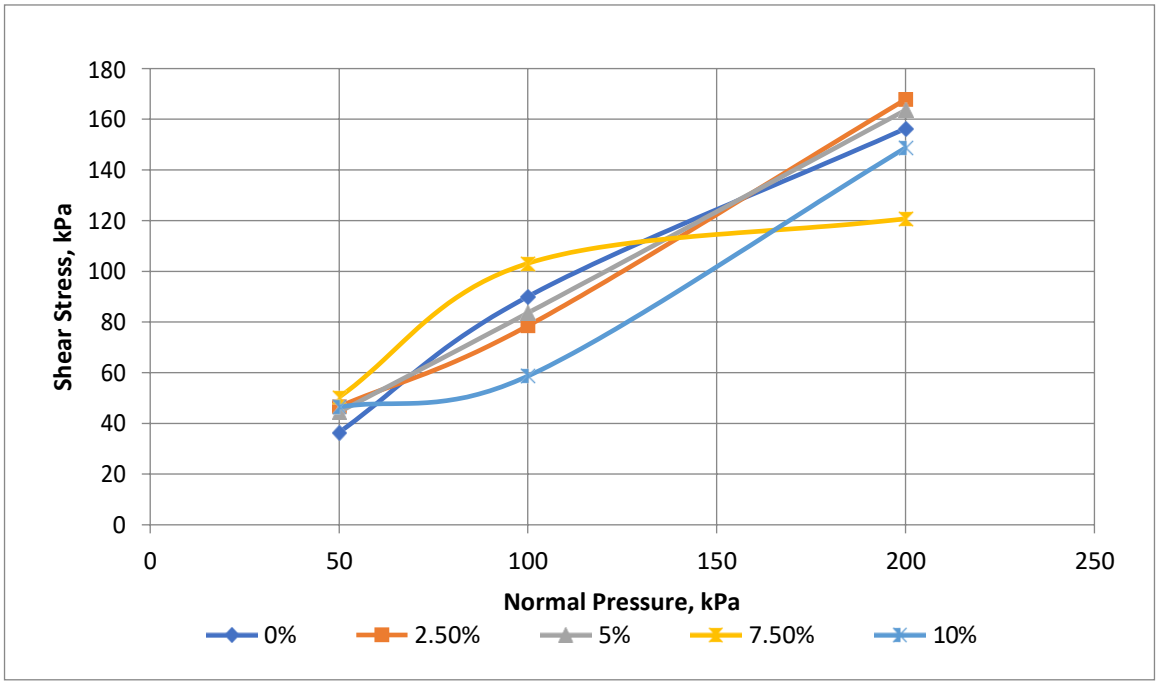

Figure 26 Variation of Stress vs Normal Pressures for different percentages of tire crumbs for Site 5 Soil Sample

5.3 UNCONSOLIDATED UNDRAINED TRIAXIAL TEST

The variation of deviatoric stress with percentage of tire crumbs in the mixture for various confining pressures on Site 1 soil sample is shown in Figure 27. The influence of tire content can be noticed by the significant increase in the deviatoric stress value, especially when the confining pressure is 100kPa at 10% tire crumbs. There is an overall steady increase in deviatoric stress with the increase in percentage of tire crumbs at all confining pressures. The variation of deviatoric stress vs normal pressure for 2.5% and 5% tire crumbs follows a very similar trendline to that of pure soil. There is an initial increase in deviatoric stress as the tire crumbs percentage increases, but at higher confining pressure, a substantial decrease in deviatoric stress is observed.

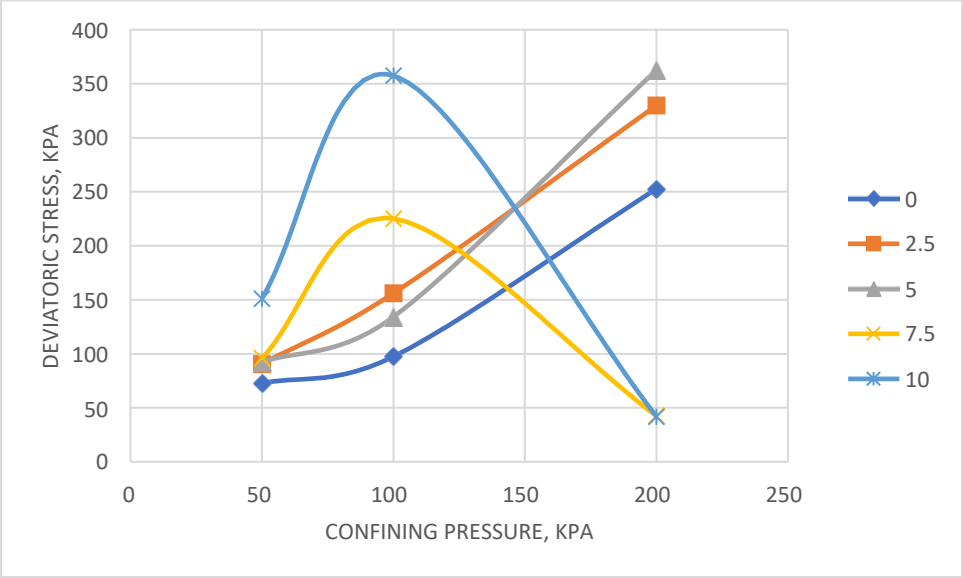

Figure 27 Variation of deviatoric stress with confining pressures for different percentage of tire crumbs for Site 1 soil sample

The Site 2 soil sample showed an overall increase in deviatoric stress value for the soil-tire crumb mixture when compared to pure soil. This increase was observed up to a percentage of 7.5%. The variation was very similar to the pure soil at 7.5% in particular. This variation is shown in Figure 28. The deviatoric stress values for STCM at 10% tire crumbs was higher than the pure soil at 50kPa and 200kPa, but it was substantially low at a confining pressure of 100kPa. The optimum percentage of tire crumbs based on the variation would

hence be 7.5%, as the variation was very similar to that of pure soil, with a steady increase in strength of STCM at all confining pressures.

Soil sample from Site 3 site showed an initial decrease in deviator stress for initial percentages of tire crumbs in STCM. This was followed by an increase in deviatoric stress

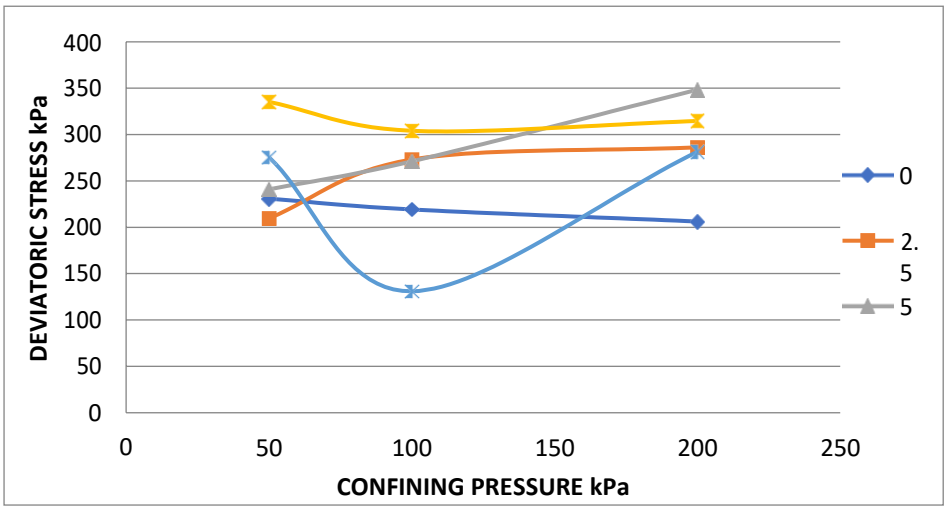

Figure 28 Variation of deviatoric stress with confining pressures for different percentage of tire crumbs for Site 2 soil sample

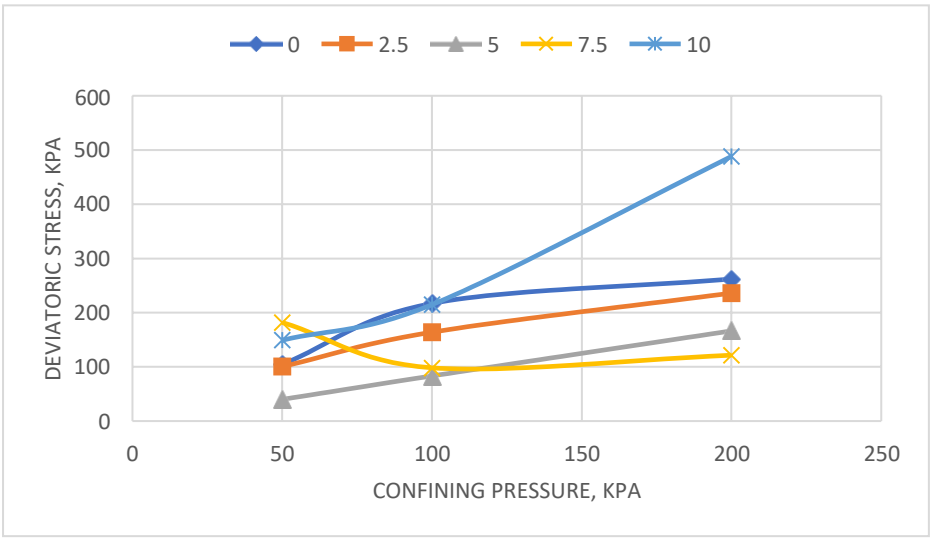

Figure 29 Variation of deviatoric stress with confining pressures for different percentage of tire crumbs for Site 3 soil sample

for all the confining pressures. This late increase in stress was observed to be significant when the percentage of tire crumbs used was 10%. This variation is shown in Figure 29.

The Site 4 soil sample showed an overall decrease in deviatoric stress value for the soil-tire crumb mixture when compared to pure soil. This decrease was observed at higher confining pressures. This variation is shown in Figure 30. The deviatoric stress values for STCM at 2.5% tire crumbs was higher than the pure soil at 50kPa and 200kPa, but it was low at a confining pressure of 100kPa. The optimum percentage of tire crumbs based on the variation would hence be 2.5%, with a steady increase in strength of STCM at all confining pressures.

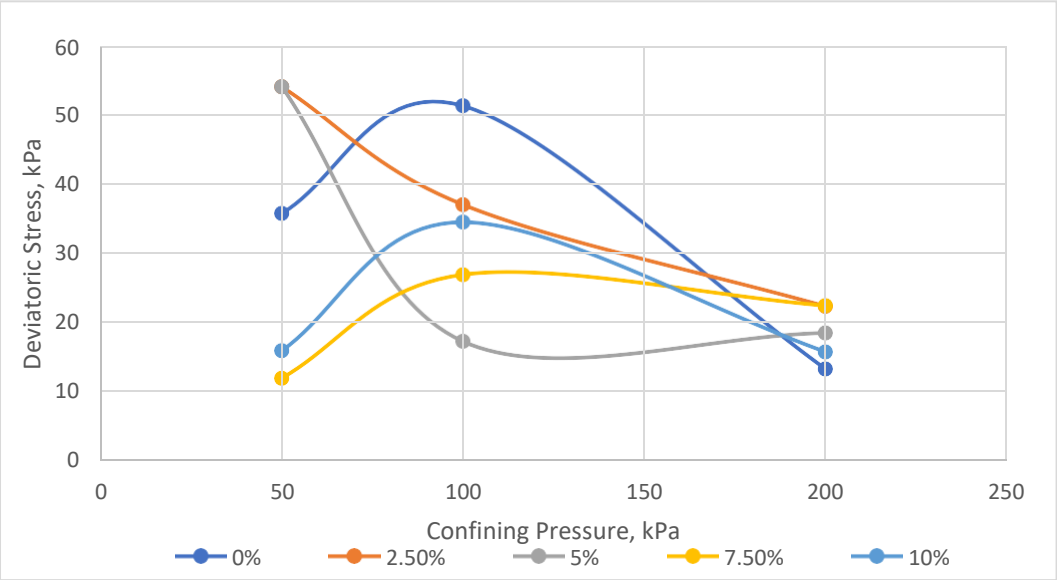

Figure 30 Variation of deviatoric stress with confining pressures for different percentage of tire crumbs for Site 4 soil sample

Soil sample from Site 5 site showed an initial decrease in deviator stress at 50kPa confining pressure. This was followed by an increase in deviatoric stress for higher confining pressures when the tire crumb percentages were 2.5% and 5%. This late increase in stress was observed to be significant when the percentage of tire crumbs used was 2.5%. This variation is shown in Figure 31.

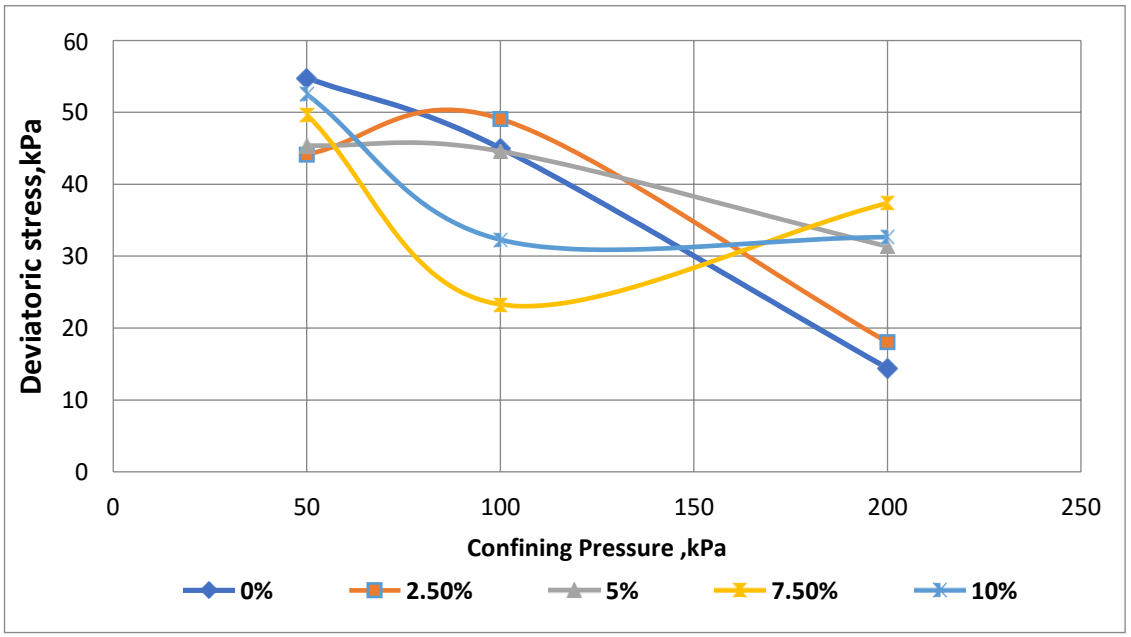

Figure 31 Variation of deviatoric stress with confining pressures for different percentage of tire crumbs for Site 5 soil sample

5.4 DUCTILITY AND ENERGY ABSORPTION

The values of brittleness index and energy absorption capacity of STCM for varying percentages of tire crumbs are summarized in Table 4.

5.4.1 Ductility

Ductility can be determined by finding brittleness index. As the brittleness index approaches zero, failure tends to become more ductile. Brittleness Index (BI) was found using the equation defined by Bishop (1967) which was stated earlier. For the Site 1 soil sample, the brittleness index for pure soil was found to initially decrease followed by a substantial increase in brittleness index, showing the soil to become less ductile at higher confining pressures. The effect of tire crumbs on brittleness index on Site 1 soil sample was found to be little to nothing as there was an initial increase in brittleness index as the percentage of tire crumbs increased. This was followed by a decrease in brittleness index at higher confining pressure, thereby showing the STCM to have become more ductile.

Table 4 Ductility and Energy Absorption values of STCM for varying percentage of tire crumbs

Material	Pressure (kPa)	Site 1		Site 2		Site 3		Site 4		Site 5	
		BI	EA	BI	EA	BI	EA	BI	EA	BI	EA
Soil	50	0.16168	11.0915	0.403075	1.67777	0.11258	11.3185	0.385701	0.92842	0.03085	2.17
	100	0.05929	9.11306	0.36107	2.07577	1.31083	22.9851	0.15455	0.82245	0.22799	1.803
	200	1.06464	17.8712	0.040467	5.14877	1.31083	27.7431	0.435957	0.08248	0.09002	0.3637
Soil + 2.5% tire crumb	50	0.77183	8.3136	0.048683	10.3273	0.17614	14.681	0.2129509	0.59642	0.2123	2.0459
	100	0.77184	14.2994	0.258806	6.8074	0.09463	14.6586	0.4072593	0.32565	0.26059	2.1769
	200	0.55293	20.4996	0.139453	5.53761	0.38396	15.9281	0.4250223	0.3559	0.42993	0.5635
Soil + 5.0% tire crumb	50	0.26644	17.3144	0.192646	9.73345	0.21032	4.19716	0.5077558	0.08157	0.77413	1.3821
	100	0.32501	10.7521	0.107865	7.31931	0.00066	6.30232	0.8813236	0.18977	1.91828	1.2557
	200	0.325	29.0199	0.158537	9.6219	0.11111	12.5823	1.3654021	0.26144	0.54834	1.1777
Soil + 7.5% tire crumb	50	0.4649	13.6032	0.224516	10.312	0.09488	21.5314	0.5225498	0.25605	0.63669	2.0436
	100	0.4649	31.9539	0.344077	8.35287	0.1878	10.3378	0.4065458	0.68375	0.39465	0.6272
	200	0.4649	6.03928	0.264891	6.38228	0.09676	14.1482	0.3256633	0.38438	0.2218	1.3886
Soil + 10% tire crumb	50	0.3302	15.8558	0.06249	6.17253	0.17426	15.4262	0.4203294	0.7979	1.1657	1.5601
	100	0.3302	37.499	0.178016	1.79361	0.17424	22.2137	1.635627	0.35563	0.3393	1.1445
	200	0.3302	4.40239	0.370405	3.13397	0.17603	50.4806	0.5137507	0.28345	0.12065	1.3204

BI – Brittleness Index; EA – Energy Absorption (kJ/m^3)

Site 2 soil sample without tire crumbs showed a decrease in brittleness index at both 2.5% and 5% tire crumbs. The effect of tire crumbs was observed with the decrease in brittleness index. It was observed that at 7.5% and at higher confining pressure, the brittleness index though decreased in variation, was higher than that of pure soil. But there was a significant increase in brittleness index when the percentage in tire crumbs was 10%. This variation was very different to that observed at all other percentages of tire crumbs, where the general trend in variation was very similar when percentage tire crumbs was 2.5%, 5% and 7.5%.

Pure soil Site 3 sample showed a substantial increase in brittleness index for increasing confining pressures. The effect of tire crumbs on Site 3 soil was observed to be immensely high. There was a significant reduction in brittleness index of the STCM, suggesting the soil to have become a lot more ductile. Although there was a general reduction in brittleness index at all confining pressures at all percentages of tire crumbs, the reduction was observed to be the highest when the tire crumbs percentage was 5%.

Site 4 soil sample without tire crumbs showed a decrease in brittleness index at 2.5% tire crumbs. But there was a significant increase in brittleness index when the percentage in tire crumbs was 10%. This variation was very different to that observed at all other percentages of tire crumbs, where the general trend in variation was very similar when percentage tire crumbs was 2.5%, 5% and 7.5%.

Pure soil Site 5 didn't show much decrease in the brittleness index on the addition of tire crumbs. There was a substantial increase in the brittleness index at 5% tire crumbs. There was observed to be a decrease in brittleness index at 2.5% and 10% tire crumbs.

5.4.2 Energy Absorption

The Energy Absorption (EA) capacity of the mix is determined by the area under the stress-strain curve obtained from UU triaxial tests. This is done by finding the summation of values of products of the average of consecutive stress values with the difference of consecutive strain values. For the Site 1 soil sample, the influence of tire crumbs was found to be significant. The energy absorption capacity of the soil increased immensely with the addition of tire crumbs. It was observed that as the percentage of tire crumbs added increased, the energy absorption capacity of the soil increased. But this increase was observed to be significant from 5% to 7.5% tire crumbs. The increase was followed by a significant decrease in energy absorption capacity at higher percentages of tire crumbs at higher confining pressures.

Site 2 soil sample showed a general increase in energy absorption capacity at all percentages of tire crumbs. This increase was significant at lower confining pressures, while there was a definite increase at higher confining pressures. This increase was significant at both 5% and 7.5% tire crumbs.

It was found that the energy absorption capacity of Site 3 soil increased only at 10% tire crumbs. While there was a decrease in energy absorption of the STCM in initial tire crumb percentages, for all confining pressures, the increase in energy absorption capacity was found to be significant at higher confining pressure at 10% tire crumbs.

For the Site 4 soil sample, the influence of tire crumbs was found to be significant, especially at higher confining pressures. The energy absorption capacity of soil decreased

at lower pressures, while the decrease was less at 7.5% tire crumbs at 100kPa pressure. The increase was found to be the most at 2.5% tire crumbs at 200kPa.

There was a substantial increase in energy absorption capacity for Site 5 soil sample. The increase was the highest at 2.5% tire crumbs, especially at lower confining pressures. The increase was for all the confining pressures.

Based on the results obtained, the optimum percentage of tire crumbs for Site 1, Site 2, Site 3, Site 4 and Site 5 soil was found to have been 5%, 7.5%, 10%, 2.5% and 2.5% respectively. This was done considering a betterment in all the parameters considered, which are increase in shear strength, increase in energy absorption capacity and an increase in ductility.

5.5 DEEPSOIL Analysis

5.5.1 Preparation of soil profiles

Soil profiles for different sites consisting of soil depths and its densities were prepared with the help of borehole data. The shear modulus of each layer was found using the relation given by Anbazhagan and Sitharam (2010), which is given by:

$$G_{max} = 24.28N^{0.55}$$

where *Gmax* is the maximum Shear Modulus and *N* is the SPT 'N' value.

The shear modulus of STCM layer was found using the Direct Shear curve, where the slope of the straight portion of the Stress vs Strain curve gives the shear modulus. This was done to the curve of the optimum percentage of tire crumbs soil.

The Damping Ratio for STCM layer was obtained as per the increase in energy absorption capacity at 0% tire crumbs and the optimum percentage of tire crumbs. The unit weight of the STCM was kept equal to the pure soil as the analysis was done as per weight batching. No water table condition was selected.

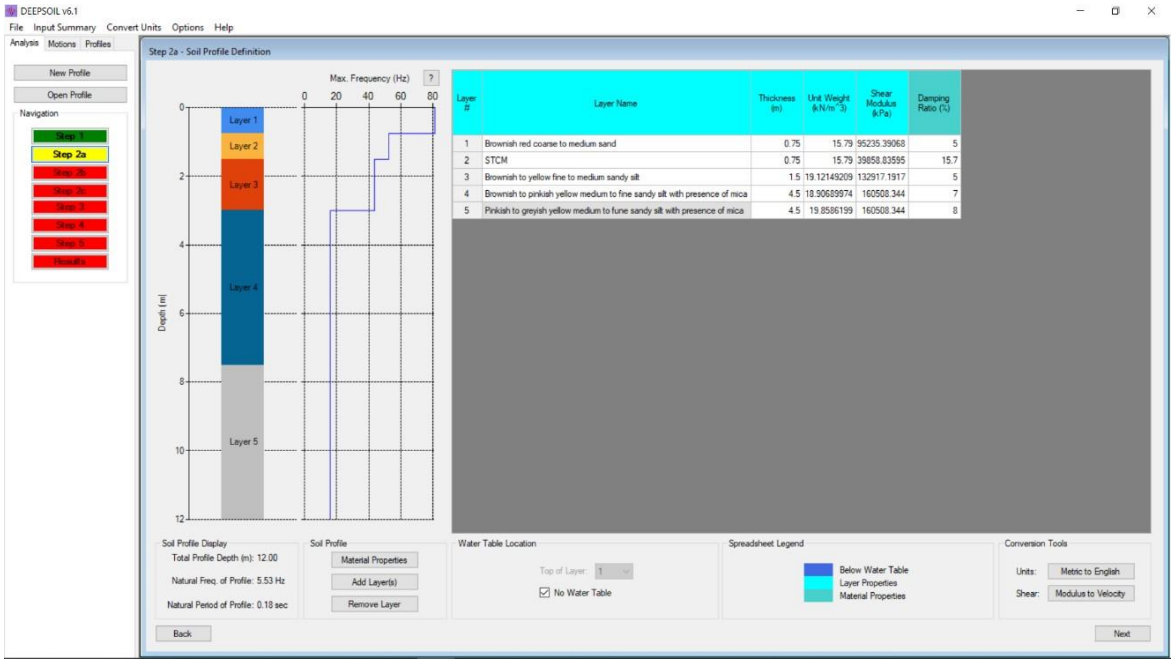

Fig. 32 Soil Profile of Site 4 Soil with STCM layer of depth 0.75m

The input motion given to the elastic half space was Koyna earthquake, which had occurred at Koynanagar, Maharashtra on December 11, 1967. The magnitude 6.6 shock hit with a maximum Mercalli intensity of VIII. This earthquake in Deccan Plateau had an intensity which has an occurrence period of 100 years. Hence, two versions of this earthquake were used for analysis – one which was not scaled down and the other which was scaled down by 0.1, which would have an occurrence period of 30 years, which would probably occur in a lifespan of a building. Hence, a high intensity strong ground motion and a low intensity ground motion are used as input motions.

Bedrock properties of Bengaluru bedrock were used for analysis, with a damping ratio of 20%. The analysis was carried out in frequency domain, with linear interpolation of time history. The analysis was carried out for all the soils, varying the depth of STCM by 0.25m.

Typical plots and output data are shown. Fig. 33 shows the PGA (g), Maximum shear strain (%) and Stress Ratio (Shear stress/Effective vertical stress) output of Site 4 Soil with STCM layer of depth 0.75m. Fig. 34 shows the Tripartite plot of response summary output of Site 4 Soil with STCM layer of depth 0.75m. Fig. 35 shows the Column Displacement output of Site 4 Soil with STCM layer of depth 0.75m.

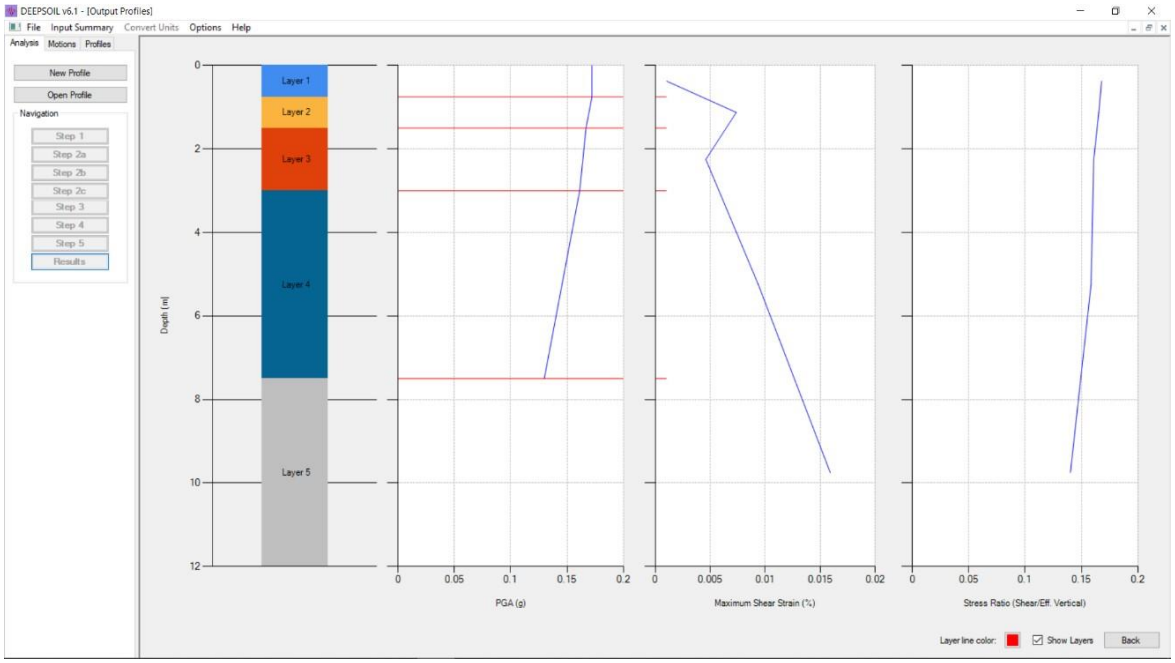

Fig. 33 PGA (g), Maximum shear strain (%) and Stress Ratio (Shear stress/Effective vertical stress) output of Site 4 Soil with STCM layer of depth 0.75m

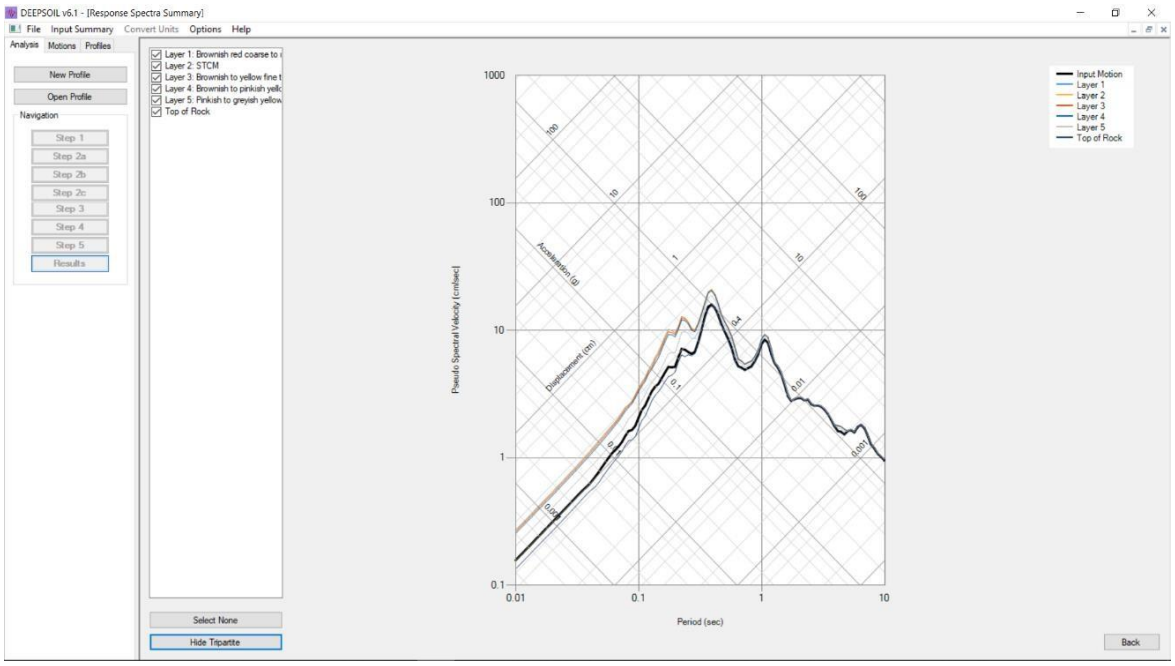

Fig. 34 Tripartite plot of response summary output of Site 4 Soil with STCM layer of depth 0.75m

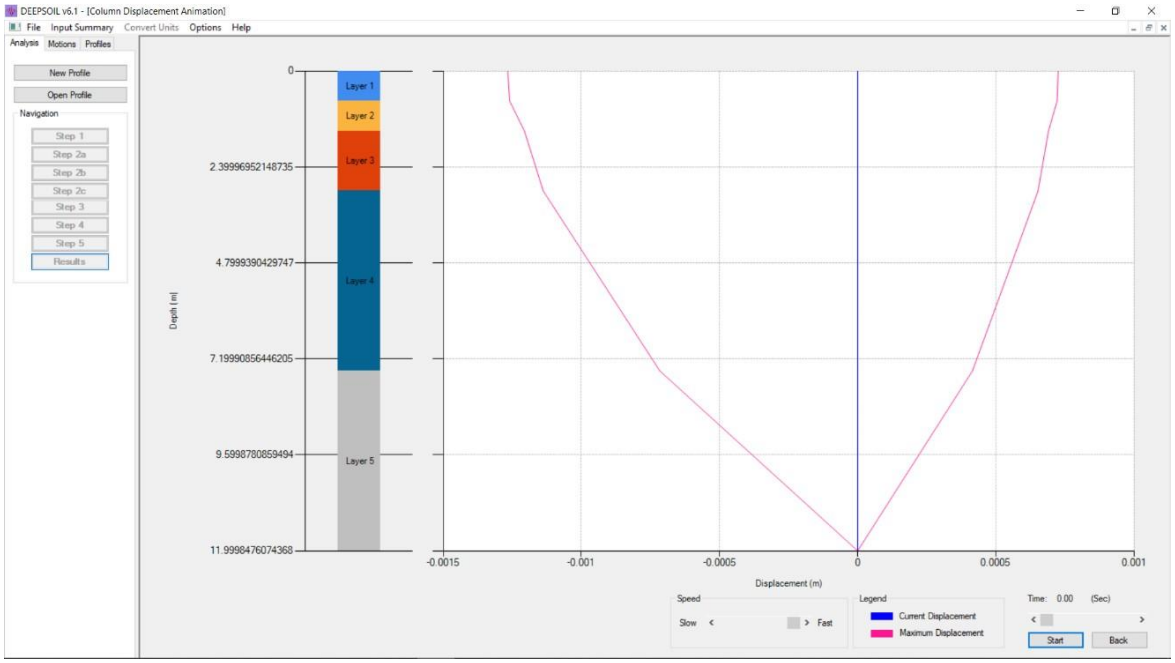

Fig. 35 Column Displacement output of Site 4 Soil with STCM layer of depth 0.75m

For easier understanding, the layers have been named as Layer 1, Layer 2 and so on. Layer 1 consists of the top layer of soil. Layer 2 is the STCM layer. Further layers include the soil present below.

Table 5 Site 1 DEEPSOIL Analysis Output

Site Specific Ground Motion – 0.36g						Site Specific Ground Motion – 0.1g					
Depth of STCM layer	Layer	Effective Stress (kPa)	PGA (g)	Maximum Displacement (m)	Maximum Stress Ratio	Depth of STCM layer	Layer	Effective Stress (kPa)	PGA (g)	Maximum Displacement	Maximum Stress Ratio
0m	Layer 1	16.25904	0.64197	0.0050387	0.618227	0m	Layer 1	16.259	0.17965	0.00141	0.173001
	Layer 2						Layer 2				
	Layer 3	46.85795	0.62818	0.0048804	0.609331		Layer 3	46.858	0.17579	0.001366	0.170511
	Layer 4	104.2204	0.60058	0.0045583	0.597109		Layer 4	104.22	0.16806	0.001276	0.167091
	Layer 5	191.9265	0.46178	0.0028136	0.522913		Layer 5	191.927	0.12922	0.000787	0.146329
0.25m	Layer 1	2.709285	0.63903	0.0050615	1.22578	0.25m	Layer 1	2.70929	0.17882	0.001416	0.343015
	Layer 2	18.96828	0.63906	0.0050596	0.611762		Layer 2	18.9683	0.17883	0.001416	0.171191
	Layer 3	46.85795	0.60095	0.0046457	0.584411		Layer 3	46.858	0.16817	0.0013	0.163538
	Layer 4	104.2204	0.57551	0.0043443	0.569974		Layer 4	104.22	0.16105	0.001216	0.159498
	Layer 5	191.9265	0.45075	0.0026789	0.497877		Layer 5	191.927	0.12613	0.00075	0.139323

Site 1 analysis results are tabulated in Table 6 as shown. The Effective Stress (kPa), PGA (g), Maximum Displacement (m) and Maximum Stress ratio, which is the ratio of shear stress to effective vertical stress, for Site 1 for two different input motions are shown below. It is observed that the effective vertical stress at Layer 1 reduced significantly on the use of 0.25m of STCM layer for both the input motions. Further, the PGA did reduce, but was not that significant. There is not a significant change observed in Maximum Displacement. With the STCM layer of thickness 1.25m, the decrease in effective stresses in improved soil was found to be 88.3367%, with the decrease in PGA and displacement being 5.03% and 6.2% respectively. At the latter specified thickness, there is a 88.88% decrease in soil strain and a decrease of stress ratio by 50.8%. Considering the overall improvement compared to other depths of STCM used, 0.25m is the optimum.

Table 6 Site 2 DEEPSOIL Analysis Output

Site Specific Ground Motion – 0.36g						Site Specific Ground Motion – 0.1g					
Depth of STCM layer	Layer	Effective Stress (kPa)	PGA (g)	Maximum Displacement	Maximum Stress Ratio	Depth of STCM layer	Layer	Effective Stress (kPa)	PGA (g)	Maximum Displacement	Maximum Stress Ratio
0m	Layer 1	13.97919	0.60942	0.0027589	0.591886	0m	Layer 1	13.9792	0.17054	0.000772	0.165629
	Layer 2						Layer 2				
	Layer 3	59.4119	0.58721	0.0025699	0.580523		Layer 3	59.4119	0.16432	0.000719	0.16245
	Layer 4	106.5905	0.41448	0.0009792	0.497941		Layer 4	106.59	0.11599	0.000274	0.139341
1.25m	Layer 1	2.329391	0.5814	0.0026027	0.721624	1.25m	Layer 1	2.32939	0.1627	0.000728	0.201935
	Layer 2	16.3086	0.58108	0.0025995	0.557303		Layer 2	16.3086	0.16261	0.000727	0.155952
	Layer 3	59.4119	0.563	0.0024363	0.545512		Layer 3	59.4119	0.15755	0.000682	0.152653
	Layer 4	106.5905	0.41159	0.0009422	0.47913		Layer 4	106.59	0.11518	0.000264	0.134077

The Effective Stress (kPa), PGA (g), Maximum Displacement (m) and Maximum Stress ratio for Site 2 for two different input motions are shown below. It is observed that there is a significant reduction in effective stress for both input motions when the STCM layer used is 1.25m thick. There is a reduction of PGA and Maximum displacement at this depth of STCM. With the STCM layer of thickness 1.25m, the decrease in effective stresses in improved soil was found to be 83.3367%, with the decrease in PGA and displacement being 4.59% and 5.66% respectively. At the latter specified thickness, there is a 79.68% decrease

in soil strain and an increase of stress ratio by 21.9%. Considering the improvement in performance of soil to the input motions, 1.25m is selected as the optimum depth of STCM.

The reduction in PGA value for Site 3 on the usage of 1.25m thick layer of STCM was 6.7%. This is shown in Table 7. There is a significant decrease in Maximum displacement

Table 7 Site 3 DEEPSOIL Analysis Output

Site Specific Ground Motion – 0.36g						Site Specific Ground Motion – 0.1g					
Depth of STCM layer	Layer	Effective Stress (kPa)	PGA (g)	Maximum Displacement	Maximum Stress Ratio	Depth of STCM layer	Layer	Effective Stress (kPa)	PGA (g)	Maximum Displacement	Maximum Stress Ratio
0m	Layer 1	15.81654	0.64088	0.0049977	0.616949	0m	Layer 1	15.8165	0.17934	0.001399	0.172643
	Layer 2						Layer 2				
	Layer 3	45.97299	0.62748	0.004844	0.608459		Layer 3	45.973	0.17559	0.001356	0.170267
	Layer 4	103.3356	0.60037	0.0045284	0.596755		Layer 4	103.336	0.168	0.001267	0.166992
	Layer 5	191.0412	0.46284	0.0027996	0.522716		Layer 5	191.041	0.12952	0.000783	0.146273
1 .25m	Layer 1	2.635555	0.59869	0.0046059	1.16418	1.25m	Layer 1	2.63555	0.16753	0.001289	0.325777
	Layer 2	18.45209	0.59876	0.0046045	0.593644		Layer 2	18.4521	0.16755	0.001288	0.166121
	Layer 3	45.97299	0.59115	0.0044972	0.557536		Layer 3	45.973	0.16542	0.001258	0.156017
	Layer 4	103.3356	0.56914	0.0042201	0.54711		Layer 4	103.336	0.15926	0.001181	0.1531
	Layer 5	191.0412	0.45523	0.0026351	0.492002		Layer 5	191.041	0.12739	0.000737	0.137679

Table 8 Site 4 DEEPSOIL Analysis Output

Site Specific Ground Motion – 0.36g						Site Specific Ground Motion – 0.1g					
Depth of STCM layer	Layer	Effective Stress (kPa)	PGA (g)	Maximum Displacement	Maximum Stress Ratio	Depth of STCM layer	Layer	Effective Stress (kPa)	PGA (g)	Maximum Displacement	Maximum Stress Ratio
0m	Layer 1	11.84178	0.62654	0.0046027	0.599729	0m	Layer 1	11.8418	0.17533	0.001288	0.167824
	Layer 2						Layer 2				
	Layer 3	38.02347	0.6168	0.0044908	0.596085		Layer 3	38.0235	0.1726	0.001257	0.166805
	Layer 4	95.38606	0.59447	0.0042351	0.589583		Layer 4	95.3861	0.16635	0.001185	0.164985
	Layer 5	183.0917	0.4706	0.0026584	0.517911		Layer 5	183.092	0.13169	0.000744	0.144929
0.25m	Layer 1	9.868547	0.58939	0.0042962	0.556545	0.25m	Layer 1	9.86855	0.16493	0.001202	0.15574
	Layer 2	21.71032	0.58319	0.0042241	0.574823		Layer 2	21.7103	0.1632	0.001182	0.160855
	Layer 3	38.02347	0.57873	0.0041569	0.547585		Layer 3	38.0235	0.16195	0.001163	0.153233
	Layer 4	95.38606	0.56407	0.0039325	0.539809		Layer 4	95.3861	0.15785	0.0011	0.151057
	Layer 5	183.0917	0.45893	0.002489	0.484894		Layer 5	183.092	0.12843	0.000696	0.13569

and effective stress values when the STCM layer used is 1.25m thick. With the STCM layer of thickness 1.25m, the decrease in effective stresses in improved soil was found to be 83.3367%, with the decrease in PGA and displacement being 6.58% and 7.84% respectively. At the latter specified thickness, there is a 68.55% decrease in soil strain and an increase of stress ratio by 88.7%. Hence, 1.25m is considered optimum here.

Table 8 shows the DEEPSOIL analysis output data. It was observed that for Site 4, the reduction in PGA, maximum displacement was maximum when the STCM layer was 0.25m thick. There was a decrease in effective stress as well when the STCM layer was 0.25m thick. With the STCM layer of thickness 1.25m, the decrease in effective stresses in improved soil was found to be 83.3367%, with the decrease in PGA and displacement being 2.49% and 2.89% respectively. At the latter specified thickness, there is a 58.55% decrease in soil strain and an increase of stress ratio by 107.07% Hence, the optimum thickness of STCM layer is 0.25m

Table 9 Site 5 DEEPSOIL Output

Site Specific Ground Motion – 0.36g						Site Specific Ground Motion – 0.1g					
Depth of STCM layer	Layer	Effective Stress (kPa)	PGA (g)	Maximum Displacement	Maximum Stress Ratio	Depth of STCM layer	Layer	Effective Stress (kPa)	PGA (g)	Maximum Displacement	Maximum Stress Ratio
0m	Layer 1	12.9367	0.6313	0.004716	0.605578	0m	Layer 1	12.9367	0.17666	0.00132	0.169461
	Layer 2						Layer 2				
	Layer 3	40.21331	0.62053	0.0045926	0.600319		Layer 3	40.2133	0.17365	0.001285	0.167989
	Layer 4	97.57609	0.59684	0.0043202	0.592289		Layer 4	97.5761	0.16702	0.001209	0.165742
	Layer 5	185.2817	0.46879	0.0027	0.519788		Layer 5	185.282	0.13118	0.000756	0.145454
1.25m	Layer 1	2.155677	0.64978	0.0051382	1.50638	1.25m	Layer 1	2.15568	0.18183	0.001438	0.421535
	Layer 2	15.09235	0.64996	0.0051373	0.608359		Layer 2	15.0924	0.18188	0.001438	0.170239
	Layer 3	40.21331	0.57671	0.0041401	0.578698		Layer 3	40.2133	0.16138	0.001159	0.161939
	Layer 4	97.57609	0.55769	0.0038775	0.566056		Layer 4	97.5761	0.15606	0.001085	0.158401
	Layer 5	185.2817	0.43757	0.002329	0.448373		Layer 5	185.282	0.12245	0.000652	0.12547

In Site 5 soil analysis, on the usage of 1.25m thick STCM, there was little to no difference in the PGA and Maximum displacement values. However, there was a significant reduction in the effective stress values. The optimum depth of STCM for Site 5 was hence concluded to be 1.25m. With the STCM layer of thickness 1.25m, the decrease in effective stresses in

improved soil was found to be 83.3367%, with the decrease in PGA and displacement being 6.21% and 8.76% respectively. At the latter specified thickness, there is a 95.78% decrease in soil strain and an increase of stress ratio by 127.2%. This is shown in Table 9.

CHAPTER 6

CONCLUSION

6.1 Conclusion

Based on all the experiments performed, analysis conducted, and the results obtained, the following may be concluded:

1. There was a definite improvement in soil properties like shear strength, energy absorption and ductility of the soil on the addition of tire crumbs to the soil.
2. The improvement was site specific – different tire crumbs percentages improved different soils
3. There was a definite decrease in Effective Stress (kPa), PGA (g) and Maximum Displacement (m), which are highly desirable, on the usage of STCM at foundation depth.
4. The optimum percentage of tire crumbs for Site 1 was found to be 5% and on performing analysis on DEEPSOIL, the optimum thickness of the STCM layer was found to be 0.25m. Hence, the best improvement of the soil foundation would be to provide 0.25m thick of STCM layer which has 5% tire crumbs.
5. The optimum percentage of tire crumbs for Site 2 was found to be 7.5% and on performing analysis on DEEPSOIL, the optimum thickness of the STCM layer was found to be 1.25m. Hence, the best improvement of the soil foundation would be to provide 1.25m thick of STCM layer which has 7.5% tire crumbs.
6. The optimum percentage of tire crumbs for Site 3 was found to be 10% and on performing analysis on DEEPSOIL, the optimum thickness of the STCM layer was found to be 1.25m. Hence, the best improvement of the soil foundation would be to provide 1.25m thick of STCM layer which has 10% tire crumbs.
7. The optimum percentage of tire crumbs for Site 4 was found to be 2.5% and on performing analysis on DEEPSOIL, the optimum thickness of the STCM layer was found to be 0.25m. Hence, the best improvement of the soil foundation would be to provide 0.25m thick of STCM layer which has 2.5% tire crumbs.

8. The optimum percentage of tire crumbs for Site 5 was found to be 2.5% and on performing analysis on DEEPSOIL, the optimum thickness of the STCM layer was found to be 1.25m. Hence, the best improvement of the soil foundation would be to provide 1.25m thick of STCM layer which has 2.5% tire crumbs.
9. The improvement of soil in all aspects does display the importance of this study, by providing an affordable and economic energy absorption and base isolation technique for an earthquake resistant structure.

6.2 Future Scope

This project deals with improving shear strength and energy absorption characteristics of a specific site and its application in vibration isolation for shallow foundations. It can further be done for deep foundations. Analytical study can be extended further to create simulation models for better results. Variation can also be done in the percentage of tire crumbs to a finer extent to obtain more accurate variation.

REFERENCES

1. Trifunac, M. D., Ivanović, S. S., & Todorovska, M. I. (2001). Apparent periods of a building. II: Time-frequency analysis. *Journal of Structural Engineering*, *127*(5), 527-537.
2. Hazarika, H., Igarashi, N., & Yamada, Y. (2011, January). Behavior of granular and compressible geomaterial under cyclic loading. In *Proceedings of Fifth International Conference on Earthquake Geotechnical Engineering*.
3. Zornberg, J. G., Cabral, A. R., & Viratjandr, C. (2004). Behaviour of tire shred sand mixtures. *Canadian geotechnical journal*, *41*(2), 227-241.
4. Gajan, S., & Kutter, B. L. (2008). Capacity, settlement, and energy dissipation of shallow footings subjected to rocking. *Journal of Geotechnical and Geoenvironmental Engineering*, *134*(8), 1129-1141.
5. Arefnia, A., Jahed Armaghani, D., & Momeni, E. (2013). Comparative Study on the Effect of Tire-Derived Aggregate on Specific Gravity of Kaolin. *Electronic Journal of Geotechnical Engineering*, *18*, 335-344.
6. Rao, G. V., & Dutta, R. K. (2006). Compressibility and strength behaviour of sand–tyre chip mixtures. *Geotechnical & Geological Engineering*, *24*(3), 711-724.
7. Anbazhagan, P., Tsang, H. H., & Mamatha, M. (2011). Earthquake Hazard Mitigation by Utilizing Waste Tyres. In *Proceeding of International Conference on Recent Innovations in Technology ICRIT 2011, 10th–12th February 2011 RIT Kottayam, Kerala, India* (pp. 59-64).
8. Gajan, S., & Kutter, B. L. (2009). Effects of moment-to-shear ratio on combined cyclic load-displacement behavior of shallow foundations from centrifuge experiments. *Journal of geotechnical and geoenvironmental engineering*, *135*(8), 1044-1055.
9. Bali Reddy, S., Pradeep Kumar, D., & Murali Krishna, A. (2015). Evaluation of the optimum mixing ratio of a sand-tire chips mixture for geoengineering applications. *Journal of Materials in Civil Engineering*, *28*(2), 06015007.

10. Anbazhagan, P., & Manohar, D. R. (2015). Energy absorption capacity and shear strength characteristics of waste tire crumbs and sand mixtures. *International Journal of Geotechnical Earthquake Engineering (IJGEE)*, *6*(1), 28-49.
11. Anbazhagan, P., & Manohar, D. R. (2015). Energy absorption capacity and shear strength characteristics of waste tire crumbs and sand mixtures. *International Journal of Geotechnical Earthquake Engineering (IJGEE)*, *6*(1), 28-49.
12. Anbazhagan, P., Mamatha, M., Soumyashree, P., Sushyam, N., Bharatha, T. P., & Vivekan, R. W. (2011). Laboratory characterization of tire crumbs soil mixture for developing low cost damping materials. *International Journal of Earth Sciences and Engineering*, *4*(6), 63-66.
13. Anbazhagan, P., Mamatha, M., Soumyashree, P., Sushyam, N., Bharatha, T. P., & Vivekan, R. W. (2011). Laboratory characterization of tire crumbs soil mixture for developing low cost damping materials. *International Journal of Earth Sciences and Engineering*, *4*(6), 63-66.
14. Panjamani, A., Ramegowda, M. D., & Divyesh, R. (2015). Low cost damping scheme for low to medium rise buildings using rubber soil mixtures. *Japanese Geotechnical Society Special Publication*, *3*(2), 24-28.
15. Akbulut, S., Arasan, S., & Kalkan, E. (2007). Modification of clayey soils using scrap tire rubber and synthetic fibers. *Applied Clay Science*, *38*(1-2), 23-32.
16. Moo-Young, H., Sellasie, K., Zeroka, D., & Sabnis, G. (2003). Physical and chemical properties of recycled tire shreds for use in construction. *Journal of Environmental Engineering*, *129*(10), 921-929.
17. Trifunac, M. D., & Todorovska, M. I. (1999). Reduction of structural damage by nonlinear soil response. *Journal of Structural Engineering*, *125*(1), 89-97.
18. Mashiri, M. S., Sheikh, M. N., Vinod, J. S., & Tsang, H. H. (2010). Scrap-tyre soil mixture for seismic protection.
19. Tsang, H. H., Lo, S. H., Xu, X., & Neaz Sheikh, M. (2012). Seismic isolation for low-to-medium-rise buildings using granulated rubber–soil mixtures: numerical study. *Earthquake engineering & structural dynamics*, *41*(14), 2009-2024.
20. Kelly, J. M. (2002). Seismic isolation systems for developing countries. *Earthquake Spectra*, *18*(3), 385-406.

21. Martelli, A., & Forni, M. (1998). Seismic isolation of civil buildings in Europe. *Progress in structural engineering and materials*, *1*(3), 286-294.
22. Xiong, W., & Li, Y. (2013). Seismic isolation using granulated tire–soil mixtures for less-developed regions: experimental validation. *Earthquake Engineering & Structural Dynamics*, *42*(14), 2187-2193.
23. Neaz Sheikh, M., Mashiri, M. S., Vinod, J. S., & Tsang, H. H. (2012). Shear and compressibility behavior of sand–tire crumb mixtures. *Journal of Materials in Civil Engineering*, *25*(10), 1366-1374.
24. Panjamani, A., & Manohar, D. R. (2013). Shear strength characteristics and static response of sand-tire crumb mixtures for seismic isolation.
25. Ghazavi, M. (2004). Shear strength characteristics of sand-mixed with granular rubber. *Geotechnical & Geological Engineering*, *22*(3), 401-416.
26. Cecich, V., Gonzales, L., Hoisaeter, A., Williams, J., & Reddy, K. (1996). Use of shredded tires as lightweight backfill material for retaining structures. *Waste Management & Research*, *14*(5), 433-451.
27. Wu, W. Y., Benda, C. C., & Cauley, R. F. (1997). Triaxial determination of shear strength of tire chips. *Journal of geotechnical and geoenvironmental engineering*, *123*(5), 479-482.
28. Ahn, I. S., & Cheng, L. (2014). Tire derived aggregate for retaining wall backfill under earthquake loading. *Construction and Building Materials*, *57*, 105-116.
29. Reddy, S. B., Krishna, A. M., & Reddy, K. R. (2018). Sustainable Utilization of Scrap Tire Derived Geomaterials for Geotechnical Applications. *Indian Geotechnical Journal*, *48*(2), 251-266.
30. Youwai, S., & Bergado, D. T. (2003). Strength and deformation characteristics of shredded rubber tire sand mixtures. *Canadian Geotechnical Journal*, *40*(2), 254-264.
31. Lee, J. H., Salgado, R., Bernal, A., & Lovell, C. W. (1999). Shredded tires and rubber-sand as lightweight backfill. *Journal of geotechnical and geoenvironmental engineering*, *125*(2), 132-141.

32. Anbazhagan, P., Uday, A., Moustafa, S. S., & Al-Arifi, N. S. (2017). Soil void ratio correlation with shear wave velocities and SPT N values for Indo-Gangetic basin. *Journal of the Geological Society of India*, *89*(4), 398-406.
33. Farrokhzad, F., & Choobbasti, A. J. (2016). Empirical correlations of shear wave velocity (Vs) and standard penetration resistance based on soil type in Babol city.